

---

This is an electronic reprint of the original article.  
This reprint may differ from the original in pagination and typographic detail.

van Rooijen, E; Dietze, M; Lotsari, E

## Employing novel wireless agricultural sensors for real-time monitoring of fluvial bank erosion

*Published in:*  
Earth Surface Processes and Landforms

*DOI:*  
[10.1002/esp.5640](https://doi.org/10.1002/esp.5640)

Published: 01/10/2023

*Document Version*  
Publisher's PDF, also known as Version of record

*Published under the following license:*  
CC BY

*Please cite the original version:*  
van Rooijen, E., Dietze, M., & Lotsari, E. (2023). Employing novel wireless agricultural sensors for real-time monitoring of fluvial bank erosion. *Earth Surface Processes and Landforms*, 48(13), 2480-2499.  
<https://doi.org/10.1002/esp.5640>

---

This material is protected by copyright and other intellectual property rights, and duplication or sale of all or part of any of the repository collections is not permitted, except that material may be duplicated by you for your research use or educational purposes in electronic or print form. You must obtain permission for any other use. Electronic or print copies may not be offered, whether for sale or otherwise to anyone who is not an authorised user.

# Employing novel wireless agricultural sensors for real-time monitoring of fluvial bank erosion

Erik van Rooijen<sup>1</sup>  | Michael Dietze<sup>2,3</sup> | Eliisa Lotsari<sup>1,4</sup> 

<sup>1</sup>Water and Environmental Engineering, Department of Built Environment, Aalto University, Aalto, Finland

<sup>2</sup>Department of Physical Geography, Georg-August-University Göttingen, Göttingen, Germany

<sup>3</sup>Section 4.6 Geomorphology, German Research Centre for Geosciences, Potsdam, Germany

<sup>4</sup>Department of Geographical and Historical Studies, University of Eastern Finland, Joensuu, Finland

## Correspondence

Erik van Rooijen, Water and Environmental Engineering, Department of Built Environment, Aalto University, P.O. Box 15200, Tietotie 1, 00076 Aalto, Finland.  
Email: [erik.vanrooijen@aalto.fi](mailto:erik.vanrooijen@aalto.fi)

## Funding information

The work for this paper was supported financially by Academy of Finland-funded projects (ExRIVER: grant number 267345; DefrostingRivers: 338480; HYDRO-RDI-Network: 337394; Green-Digi-Basin 347701; HYDRO-RI-Platform 346167) and two mobility fundings (Mobility Grant from Russia to Finland to Nikita Tananaev 333218 and mobility grant between Finland and Germany [TU Dresden] 332563) and enabled field campaigns in 2020–2022 at Pulmanki River. Also, the Department of Geographical and Historical Studies, University of Eastern Finland, Emil Aaltosen säätiö ('kohdeapuraha' in 2016), and funding from Maj and Tor Nessling Foundation (ExRIVER, grant numbers: 201300067 and 201500046; Influence of river ice and fluvial processes on river environments now and in the future, grant number: 201600042) supported Lotsari's and her team's work financially during 2013–2021. Lotsari also received from the British Society for Geomorphology (research project title 'Defrosting sedimentary systems: the impacts on the evolution and material transport of high-latitude rivers' [registered charity number: 1054260]) for pilot data gathering from Pulmanki River.

## Abstract

Bank erosion impacts sediment transport and river morphology, both important processes for river managers. Some important factors, such as timing and causes of bank erosion, are difficult to assess with established techniques. We explore the capability of smart sensors, actually developed for the agricultural sector, to measure soil moisture and temperature as well as movement in real time on banks of northern rivers in different geographical, climatological and landscape settings. Soil movement and its timing were easy to identify from the measurements, and in many cases, the reason for the onset of movement could be inferred. The sensors automatically upload data with a high temporal resolution for a long period of time, while only minimally disturbing the bank itself. However, the sensor approach has a low spatial resolution (point measurements), and therefore, complementing the measurements with approaches with a high spatial resolution, such as spatially continuous digital elevation models of differencing techniques or seismic sensors, is advised. Overall, the measurement approach using new agricultural sensors has several unique advantages and disadvantages and can be a good tool for the monitoring of river bank erosion and could lead to new insights.

## KEYWORDS

bank erosion, measurement, monitoring, sensor, soil moisture, soil scout, soil temperature

## 1 | INTRODUCTION

If you frequently walk along a river with high banks consisting of erodible material, you will notice that those banks constantly change. They collapse and retreat. These dynamics, inherent to active rivers and a necessary part of self-adjustment of the fluvial system, can have impacts on human societies (Best, 2019; Hutton & Haque, 2004).

Injection of eroded bank material into the stream affects sediment transport and river morphology (e.g. Kronvang et al., 1997; Neal & Anders, 2015; Sekely et al., 2002). In turn, sediment transport and river morphology are of major importance for river managers as they can affect the channel capacity and flood risk (Nones, 2019), the amount of nutrients in rivers (e.g. Green et al., 1999; Kronvang et al., 1997; Sekely et al., 2002) and lotic habitats (Rachelly

This is an open access article under the terms of the [Creative Commons Attribution](https://creativecommons.org/licenses/by/4.0/) License, which permits use, distribution and reproduction in any medium, provided the original work is properly cited.

© 2023 The Authors. *Earth Surface Processes and Landforms* published by John Wiley & Sons Ltd.

et al., 2021; Staentzel et al., 2020; van Rooijen et al., 2022), among others. Therefore, it is important to know the amount and timing of sediment supplied to the river. The timing may for example impact fluvial habitats (van Rooijen et al., 2022), or the management of hydraulic structures (Zhang et al., 2017). Monitoring and further modelling of bank erosion are thus crucial.

In recent years, the development of digital twins, virtual representations of physical systems (such as rivers) that help improve decision-making through real-time data acquisition and modelling, has gained research interest (Tao et al., 2022). More recently, this interest has also spilled over into the field of fluvial hydraulics and river management (Moteki et al., 2022; Spreitzer et al., 2022). In essence, this is an extension of the modelling that has historically been carried out to better assess river systems (c.f. Pedersen et al., 2021), including bank erosion (e.g. Darby et al., 2007; Langendoen & Simon, 2008; Osman & Thorne, 1988; Rinaldi et al., 2008; Simon et al., 2000). In order to adequately model bank erosion, empirical data on the amount and especially the timing of bank erosion are crucial (Lawler, 2005, 2008) to obtain calibration and validation data. Additionally, soil moisture (Casagli et al., 1999; Wynn et al., 2008; Yumoto et al., 2006) and temperature (Lawler, 1986; Wynn et al., 2008; Yumoto et al., 2006) have to be measured with sufficiently high temporal and three-dimensional spatial resolution (Lawler, 2005) and are, together with fluvial parameters (e.g. shear stress), the basis of bank erosion processes (Couper & Maddock, 2001).

In cold climatic regions, such as in northern high latitudes, bank erosion is more complex because of the snow- and ice-covered winter season. Freeze–thaw processes are more common, which can cause bank erosion directly or make other erosional processes occur more easily (Chassiot et al., 2020; Frauenfeld et al., 2007), and also, the effect of river ice cover and breakup should be considered (Chassiot et al., 2020; Vandermause et al., 2021). At the same time, climate change affects these areas more than other areas (IPCC, 2022).

Multiple measurement approaches have been developed in the past to measure bank erosion and its forcing parameters, such as (photo electronic) erosion pins, digital elevation model (DEM) of differencing approaches, repeated cross profiling, marked pebbles, tension-piezometers, various sensors with dataloggers, lateral flow collection flumes, electrical resistivity tomography (ERT), markers and manual measurements (for details, see Table 1). Note that in Table 1, only the methodologies for short to intermediate timescales are shown (timescale of interest up to several decades and a resolution of 1 year or higher); other methods for longer timescales have also been applied (see Lawler, 1993). Furthermore, some of the approaches can be subdivided into multiple approaches, such as the Comparison of Digital Terrain Models (DTMs), which can be subdivided into the multiple different approaches in which the DTM is obtained, or the sensors with data loggers, where many different parameters can be measured (see, e.g. Matsuoka, 1994, 1996, 2001, 2005), although sensors other than those for soil moisture and temperature have rarely been used in river banks (but see, e.g. Yumoto et al., 2006). It must also be noted that even more approaches exist that can measure hillslope erosion or its forcing parameters (Lekshmi et al., 2014; Stroosnijder, 2005), but these have not yet been used in river bank erosion studies. Seismic sensors are another approach to measuring riverbank erosion, although they have not yet been applied as such

(but see Feng et al., 2019). They can sense ground motion caused by meteorological and Earth surface processes, like rain drop impacts, pebble impacts on the riverbed during sediment transport events and gravitational mass wasting events on hillslopes (Cook & Dietze, 2022). Seismic sensors can be installed at a safe distance and sense hillslope activity as well as trigger processes at a sub-second temporal resolution (e.g. Dietze et al., 2020).

Often several of these measurement approaches are combined (e.g. Casagli et al., 1999; Fox et al., 2007; Prosser et al., 2000; Veihe et al., 2011), which allows the investigator to combine the advantages of different approaches. However, many current measurement approaches (Table 1) have important limitations in terms of parameters measured together, temporal resolution, maintenance cycles and data access and impact on the measured bank during deployment and operation. In addition, none of the approaches have been used in a real-time monitoring campaign, which would have benefits for river managers and scientists alike (c.f. Meyer et al., 2019). Thus, measuring bank erosion along with its forcing parameters in real-time, at high-temporal resolution, while minimizing the bank impact, and with long maintenance cycles, could significantly advance our understanding of bank-stream interaction in river systems and complement the existing measurement approaches.

Considering this, the goal of this paper is to explore a new measurement approach that can detect both the timing of erosion as well as the forcing parameters, and which requires less frequent field visits than existing approaches. We are specifically interested in novel sensors developed for the agricultural industry, which have been refitted with a digital accelerometer as well. Of course, the sensor approach can also be used for other types of banks besides river banks.

The aim of this paper is not to supplant the current measurement and analysis approaches but rather to supplement them with novel techniques to enhance measurement and monitoring campaigns. We installed the sensors at three different sites with different geographical, climatological and landscape settings in Finland to obtain a representative view of how these sensors work in different environments. We discuss the performance, installation requirements and emerging system insights that such sensors inhere. We compare the sensors with independent measurements of river bank change detection: (1) amount of erosion from UAV-based DEMs of difference (DoD), (2) detection of timing of erosion from time-lapse pictures and videos, (3) geophysical event detection from geophones and (4) a traditional soil sensor approach for detecting moisture and temperature parameters.

## 2 | FIELD SITES

We test the sensors at three river bank sites in different geographical, climatological and landscape settings in Finland: the Pulmanki, Oulanka and Vantaa rivers (Figure 1). In addition, one collapsing palsa mire (a peat mound with permanently frozen core [Verdonen et al., 2023]) bank was considered in one of the river systems. These sites are the major test study sites of the Fresh Water Competence Centre (FWCC, <https://www.freshwatercompetencecentre.com/>) in Finland, where research infrastructure and new measurement solutions are developed to create digital twins of freshwater environments

TABLE 1 Overview of approaches previously used to measure and monitor river banks.

Measurement approach	Description	References	Monitored parameters	Temporal resolution	Spatial resolution	Notes
Erosion pins	Pins firmly attached in the bank with markers which can be read to identify the change in bank position	Lawler, 1993; Thorne, 1981; Veihe et al., 2011	Erosion/deposition	As often as the investigator goes to the field to read the pins	As the pins are spaced, often several decimetres to meters apart	Can impact the bank itself
Photo electronic erosion pins (PEEP)	Multiple photovoltaic cells in a line in a tube firmly attached into the bank. The number of cells exposed to light identifies the location of the bank. Recent versions also include temperature sensors	Lawler & Leeks, 1992; Lawler, 2005, 2008	Erosion/deposition, temperature	Depends on set-up, typically in the order of 10 min	As the pins are spaced, often several meters apart	Can impact the bank itself. Has problems when photovoltaic cells are covered, e.g. by vegetation or snow. Potential to turn it into a real-time measurement approach
Comparison of Digital Terrain Models (DTMs) <sup>a</sup>	Multiple DTMs are obtained using terrestrial laser scanning, terrestrial or boat-based photogrammetry or structure from motion technique. The DTMs are then compared to obtain the location and amount of erosion and deposition.	Barker et al., 1997; Brasington et al., 2000; Duró et al., 2018; Hamshaw et al., 2019; Leyland et al., 2017; Sekely et al., 2002; Thoma et al., 2005	Erosion/deposition	As often as the DEMs are available	Similar to the spatial resolution of the obtained DTMs, usually in the order of centimetres	DTMs can be obtained in many different manners.
Repeated cross-sectional profiling	Multiple cross-sectional profiles are compared to obtain the locations where erosion or deposition occurred.	Prosser et al., 2000	Erosion/deposition	As often as the cross profiles are available	Spaced as the cross-sections	Depending on the ground profiler, the bank itself may be affected.
Marked pebbles	Pebbles are marked (e.g. using paint) and placed on the bank at specific locations. After some time has elapsed, the pebbles can be collected and their locations compared to the original locations.	Thorne, 1978	Erosion/deposition	As often as the pebbles are collected	As the pebbles are spaced	

TABLE 1 (Continued)

Measurement approach	Description	References	Monitored parameters	Temporal resolution	Spatial resolution	Notes
Tensiometer-piezometers	Pipes into the ground in which the water head and matric suction are measured	Casagli et al., 1999; Rinaldi et al., 2004	Soil moisture and groundwater flow	Dependent on set-up, usually in the order of minutes to hours	At the location of each pipe	Can impact the bank itself
Sensors with dataloggers	Sensors, often buried, that measure a parameter and are connected with wires to a data logger	e.g. Yumoto et al., 2006; Veihe et al., 2011; Kaczmarek et al., 2021	Depends on the sensors installed, usually soil moisture and temperature, but many different parameters are possible such as frost heave	Dependent on set-up, usually in the order of minutes to hours	At the location of each sensor	Can impact the bank itself, many different types of sensors are possible, each measuring different parameters
Lateral flow collection flumes	A triangular pan is inserted into the bank and collects the water and sediment washed out of the bank. The amount that is collected over a certain time span is weighed.	Fox et al., 2007; Wilson et al., 2007; Midgley et al., 2013	Subsurface flow and seepage erosion	Dependent on bottle size and time in the field	As the pans are spaced	Requires investigator to be present, can impact the bank itself. Taking the measurements may be hazardous under some conditions. Is prone to clogging
Electrical resistivity tomography (ERT)	Electrical resistivity of soil is measured using electrodes. The resistivity is dependent on soil moisture, consistency and temperature. If two are known or can be approximated, the other can be obtained.	Sjödahl et al., 2008; Jodry et al., 2019; Weller et al., 2014	Soil moisture or internal erosion	Normally maximum of once a day	Order of decimetres to meters	Mostly used in levees
Markers	Markers (e.g. stakes) are placed at the top of the bank. The distance from the bank top to these markers is measured. The difference in distance identifies erosion rate of the bank.	Bernatchez & Dubois, 2008	Erosion	As often as the distance from the marker to the bank top is measured	As the markers are spaced	
Manual Measurements	Measurements done by the investigator during fieldwork.	e.g. Yumoto et al., 2006	Many different parameters are possible (e.g. soil moisture), but most often used for soil properties	As often as the investigator takes the measurement	As the investigator spaces the measurement	

<sup>a</sup>Note that in this work, a DEM is used instead of a DTM, because the investigated area is of bare ground.

and to further their application. FWCC was inaugurated in 2022 by the University of Turku, Aalto University, University of Oulu, Finnish Environmental Institute and Finnish Geospatial Research Institute of the National Land Survey of Finland.

The subarctic Pulmanki site (Figure 1e) in the far north of Finland is a well-studied meandering river with high outer banks (Lotsari et al., 2014, 2019, 2020). The investigated bank is approximately

300 m long and 18 m high and has a slope of about  $36^\circ$ , close to the friction angle of the soil material (Lotsari et al., 2020). It is strongly erosional, exceeding retreat rates of 1 m/a at times. Erosion is concentrated at the downstream part of the bank (Lotsari et al., 2014, 2020), where groundwater seepage is abundant (Lotsari et al., 2020). Shrubs and alpine birch are present on top of the bank (Lotsari et al., 2014), but the bank itself is bare soil, with occasional tufts of grass. The top

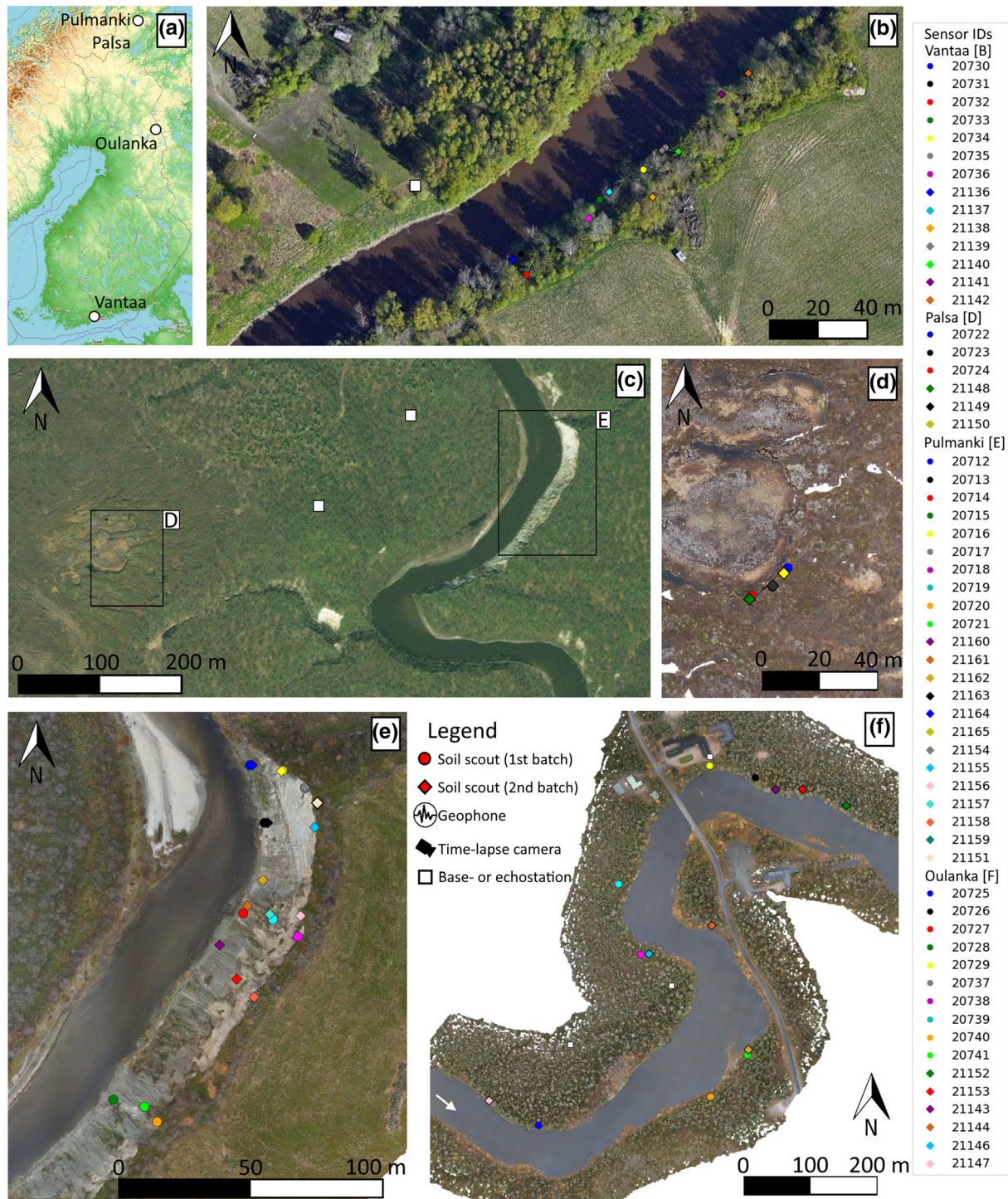


**FIGURE 1** Overview of the field sites in this study. (a) Map of Finland with the locations of the field sites marked. (b) Overview of the Vantaa river bank field site. (c) Overview of the locations of the palsa and Pulmanki bank site with their base and echo locations. (d) Overview of the palsa field site at Pulmanki river watershed. (e) Overview of the Pulmanki river bank field site, including the camera locations and the location of the geophone. (f) Overview of the Oulanka river bank field site. The coloured markers indicate the locations where soil sensors are installed, the colours of which match the colours in Figures 3–6. The circular markers were the first to be installed, followed by the diamonds. [Color figure can be viewed at [wileyonlinelibrary.com](http://wileyonlinelibrary.com)]

1.5 m of the bank consists of loose sand, which lies on top of 15 m of laminated fine sandy silt and clayey silt (Lotsari et al., 2020). The surrounding area is used for reindeer herding, and approximately 1 km upstream starts the Kaldoaivi Wilderness Area. As such, the bank is occasionally disturbed by reindeer (evidenced by hoofprints). For more information about the investigated bank and its composition, see Lotsari et al. (2020). In addition to this bank, we also investigated a collapsing palsa mire close to the Pulmanki river channel (Figure 1d). We specifically investigated the movement of the bank of its approximately 1.5 m deep thermokarst pond (Figure 1d). These thermokarst ponds are common in circumpolar regions and thus affect the hydrology of river systems (Bouchard et al., 2016). The movement of the bank of a thermokarst pond is more continuous than the event-based bank collapses. Thus, it gives important knowledge on the sensor system's ability to monitor different types of bank collapses.

The Oulanka site (Figure 1f) is a 1350-m-long meandering reach in the strongly vegetated Oulanka National Park in the North-East of Finland, right next to the Kiutaköngäs meteorological station. The terrain is uneven, with undulating, hilly topography and slopes of up to 40°. The soil consists of moraine overlain with a thin layer (<10 cm) of topsoil (Vesa-Matti Kleemola, research engineer at Oulanka research station, personal communication, 9/11/2022). Groundwater flow is present at the downstream area of the field site (H. Marttila, Prof. at University of Oulu, personal communication, 25/8/2022).

The Vantaa river (Figure 1b) is in the south of Finland and flows through the Helsinki metropolitan area. The investigated bank is just upstream from the urban areas in an agricultural area approximately 2.5 km from Helsinki–Vantaa airport. The bank is strongly vegetated, is approximately 200 m long and has a mild slope (approximately 22°). The river is straight with strong anthropological influences (e.g. agriculture).

### 3 | METHODS

At the different field sites, we deployed beta versions of a telemetric sensor system developed by a company called Soil Scout (based

in Finland), mainly for application in the agricultural industry. The system consists of a base station with a telemetry unit and a varying number of individual sensors (from here on called 'soil scouts') that connect to the base station via an underground single-ended monopole antenna (USEMA; Figure 2) over the 869-MHz radio frequency (Tiusanen, 2013). The base station uploads the arriving sensor data packages over the mobile phone network to a cloud storage service, from where it can be downloaded at regular intervals.

The sensors (Figure 2) have dimensions of 13 × 6 × 3 cm. On one end of the sensor is the USEMA and on the other a 3-prong integrated capacitive (moisture content) and resistive (electrical conductivity/salinity) sensor, whereas, in the middle, the battery and a temperature sensor are placed. After deployment by shallow burial in the ground, they require no field maintenance during their anticipated lifetime. Most of the time, the sensor is 'hibernating', and once every 20 min, it wakes up, takes a measurement, transmits it and goes back into hibernation mode. The data are automatically transmitted to the base station at 20-min intervals. Standard versions measure soil moisture, temperature and salinity, with accuracies of 2%, 0.1°C and 0.2 dS/m, respectively (Soil Scout, 2022). The temperature's resolution depends on the temperature and ranges between 0.25°C between −10°C and 10°C and 1.0°C at temperatures below −10°C.

The radio signal is transmitted in the plane around the x-axis (see Figure 2a) and is transmitted through the soil and air; at the soil–air interface, the signal refracts (Tiusanen, 2005, 2013). This signal is picked up by either an echo, which repeats the data package, or a base station. The echo and base stations were installed on poles less than 300 m from the soil scouts. The echo and base stations can either run on the built-in solar panel, a lead-acid battery, or be plugged into the electrical grid.

In this work, we used beta-versions of new soil scouts which are equipped with an additional digital accelerometer (accuracy 0.004 g). It measures the angular positions around the x-, y- and z-axes (Figure 2a). This sensor allows the detection of soil movement, assuming that the soil scout will only move if the soil around it moves.

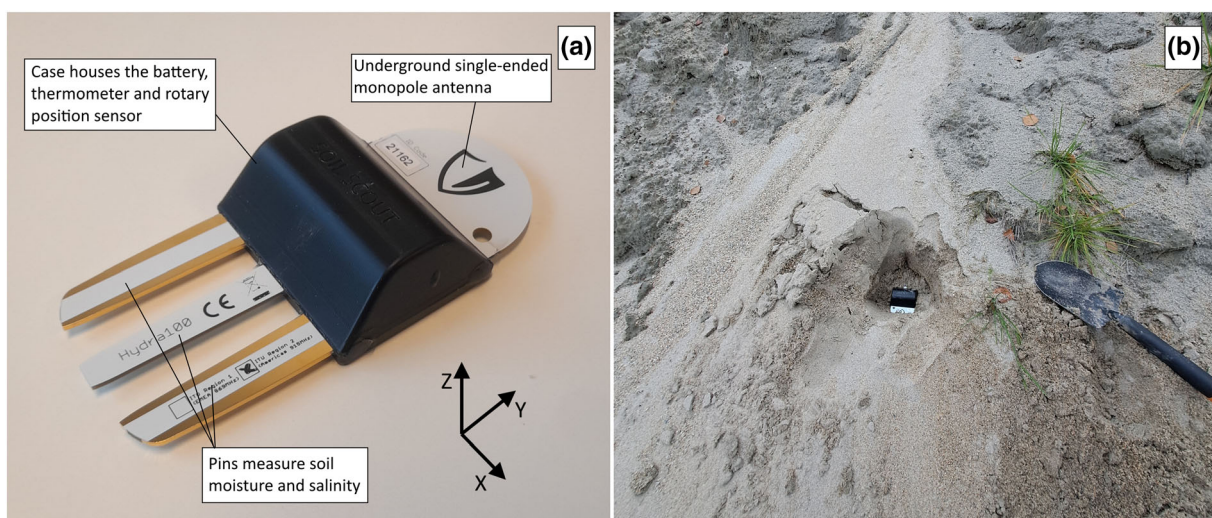


**FIGURE 2** Example of a soil scout. (a) A soil scout with indication of its parts and the axes of rotation for the digital accelerometer. (b) A soil scout during installation in the bank. [Color figure can be viewed at [wileyonlinelibrary.com](http://wileyonlinelibrary.com)]

### 3.1 | Installation procedure of the soil scouts

First, the base stations and potential echo stations were installed. Then, as part of the installation procedure, sediment samples were collected from the locations of each sensor, for bulk density and grain size analyses purposes, which are discussed elsewhere, by pushing a pipe with an inner diameter of 7 cm into the ground, digging it out, measuring the soil volume and packing, sealing and saving the soil in a plastic bag for later analysis in the laboratory. The hole was then deepened or filled in so that it was approximately 10–20 cm deep, which is the ideal installation depth. The soil scout was then placed horizontally into the hole, with the antenna pointing to the nearest echo or base station. Finally, the hole was filled in using surrounding soil. During the filling process, care was taken to maintain a potential layering of the soil if it was present.

At the Pulmanki site, 10 sensors were installed (Figure 1e) on 19 May 2022. The base station was set up on top of a hill, which is the location with the best mobile phone connection in the area. Four sensors were installed at the foot of the bank close to the water level in visually different soils. The other six sensors were installed close to the top and in the middle of the bank approximately above three of the installed sensors at the bottom. Only locations that could be safely reached were considered, and care was taken to disturb the bank as little as possible during installation. An echo was installed on another hill, located close to the palsa mire, and three sensors were installed at the palsa mire site (Figure 1d), in an area where soil movement was expected.

At the Vantaa site, seven sensors were installed (Figure 1b) on 22 June 2022. The base station was set up at the opposite side of the bank. Because of the large amount of vegetation, roots prevented the installation at many locations. As such, sensor locations were determined based on the locations where it was possible to dig holes.

At the Oulanka field site, 10 sensors were installed (Figure 1f) on 10 July 2022. The base station was plugged into an outlet and an echo was placed on top of a hill. After the installation of the sensors, it was found that the data packages of some sensors were not always received and uploaded to the cloud storage; therefore, an additional echo station was installed. The dense vegetation (tree roots) and underlying soil type (moraine) made it difficult to dig holes, and locations were chosen based on both expected groundwater effects and ease of digging.

During these initial tests, fine-tuning of the sensors was needed before reaching the final state for long-term measurements. Because of initial software malfunction, soil moisture and salinity data were not properly transmitted by the sensors (e.g. only temperature and angle measurements were properly received). Therefore, it was decided that at the Vantaa and Oulanka sites, 'standard' soils scout sensors measuring soil moisture content, temperature and salinity would be installed next to (e.g. 10–20 cm away from) the adapted soils scout sensors. Additionally, on 7 September 2022, 27 September 2022, 28 September 2022 and 4 October 2022, additional beta-version sensors with correct software were installed at the Vantaa, Pulmanki bank and palsa and Oulanka field sites, respectively. At each site, at least one soil scout was installed close to one installed previously (Figure 1). This way there was data from old and new versions for verifying the

similarities. Others were installed at different locations to increase the spatial coverage of the measurements.

Directly after installation, the soil scout started sending data. Because the base and echo stations were installed first, it was possible to see if the individual sensors were connecting properly to the base station within 20 min after installation in the ground on a smartphone in the field. With exception of sensors 20727, 20740 and 20741, all sensors connected, although for some a reduced number of data packages arrived. All of these sensors were in the Oulanka field site, as the topography of the region was more difficult for orienting the sensors directly towards the echo or base. One additional echo was installed at the Oulanka field site to ensure proper connection of soil scouts 20740 and 20741.

### 3.2 | Soil data analysis from the sensors

The sensors provide direct information on temperature, salinity and moisture in the soil, as well as inclination of the sensors. However, net erosion of the overburden material can also be accessed indirectly. Following the approach of Hautala and Tiusanen (2007), we exploited the phase shift information of the temperature time series. Because the downward propagation of the surface temperature signal is a diffusive process, one can interpret a phase shift as increasing or decreasing depth of the soil scout relative to the surface, hence deposition or erosion of the overburden material. Instead of identifying the phase shifts between air temperature and all soil scout temperature curves, we calculated the mean timing of the highest as well as the lowest daily soil temperatures across all soil scouts as reference for our phase shift analysis. This increases the robustness of the data, because air temperature can have multiple peaks per day, whereas soil temperature usually only has one peak. The results are reported after a 9-day running average was applied to smooth the results for ease of interpretation.

### 3.3 | Reference data

The obtained soil scout data were compared with four independent control data sets: DoD, time-lapse imagery, geophone survey of mass wasting activity, and further moisture and temperature measurements. These data sets were not all obtained during the same time period. DoD analysis provides precise information on the location and volume of failed material but leaves a large uncertainty as to when those failures have happened. The DEMs used in the DoD analysis were generated from UAV-based RGB-photogrammetric Structure from Motion analyses. UAV surveys were undertaken within the same week as the installation of the soil scouts and the additional soil scouts. At the Vantaa field site, UAV flights were not allowed because of the proximity to Finland's largest airport, Helsinki-Vantaa. The aerial photos were post-processed using Agisoft Metashape Professional V1.8.4 (following the approach of Over et al., 2021), and based on ground control points (measured using a Trimble R10 RTK-GNSS) and the RTK-GNSS location of each photo (drone had connection to Trimnet Virtual reference station), to obtain DEMs for the banks. Errors of these DEMs are less than the accuracy of the ground control points ( $\pm 5$  cm), which were not used in the calibration of the DEM. Elevations for the underwater

portion of the field site were not resolved. For more information on the DoD analysis, see the Supporting Information.

Time-lapse cameras (Burrel, Finland, #810017, 12MP images) were located on the opposite side of the river from the Pulmanki bank site (Figure 1e). These cameras were installed in 2013 and have continuously gathered photos with 20-min intervals since at least 2015 (Lotsari et al., 2019). The analysis of the data is limited to the period until 26 September 2022, when the data from the cameras were downloaded. The area visible on the cameras covers the most downstream area of the bank (sensors 20712, 20713, 20717 and 20716; e.g. blue, black, grey and yellow in Figure 1e, respectively).

A seismometer station was deployed at the Pulmanki site for 108 days in 2018. The main goal was to increase the temporal information on bank activity as constrained by the time-lapse imagery, not to detect bank failures, a nevertheless possible application if more than a single station would be used. The geophone (SENSOR, the Netherlands, PE6/B 4.5 Hz 3-component sensor, sensitivity: 28.8 Vs/m) was installed oriented to the North on top of the bank (Figure 1e), in a 50-cm-deep hand-dug pit. The ground motion signals were registered by a Digos DataCube<sup>3</sup>ext data logger, recording at 200 Hz with a signal preamplification factor of 32. The logger was powered by a 12-V lead battery, allowing for a continuous record span of 108 days. After recovery of the station, the logger data were used to compute a spectrogram (Welch method with 20-min-long non-overlapping windows) for the entire deployment period, using the R package *eses* v. 0.7.2 (Dietze, 2018), to check the completeness and validity of the data. To analyse bank failure events, we imported the seismic data for the period between two camera shots that witnessed a bank surface change and inspected the spectrograms for typical signatures of hillslope activity: emergent signals that last between 5 and 20 s, that show a cigar shape indicative of an emerging granular flow of unconsolidated material, with a typical broadband frequency signature, and whose seismic waveforms are absent of characteristic distinct P- and S-wave phases indicative of earthquakes, or series of short pulses of ground motion indicative of footsteps or impulsive impacts (Cook & Dietze, 2022; Hibert et al., 2011).

The data from the soil scouts are compared with the data obtained from two traditional soil moisture (Decagon Devices, United States, ECH<sub>2</sub>O EC5, accuracy:  $\pm 3.1\%$ ) and temperature sensors (Onset, United States, S-TMB-M002, accuracy:  $\pm 0.2^\circ\text{C}$ ) attached to a HOBO datalogger (HOBO, United States, #H21-002) first installed in the Pulmanki field site in spring 2017 (Lotsari et al., 2020). Temperature data can be compared with the soil scout temperature data installed at the Pulmanki site, between 19 May 2022 and 28 September 2022 (installation of soil scouts and last chance to offload data from hobo, respectively). Soil moisture data cannot be directly compared with the soil scout soil moisture data because of the aforementioned software issue of the soil scouts.

## 4 | RESULTS

### 4.1 | Data obtained with the soil scouts

The soil scout data suggests that movement of the banks has occurred at all field sites during the investigation period

(Figures 3–6). Rotation of the sensors predominantly occurred around the x- and y-axes, and little movement occurred around the z-axis. Especially at the Pulmanki site, soil movements were frequent (Figure 5c–e), and one sensor was even lost shortly after installation (soil scout 20713 on 25 May 2022; Figure 5c–e); just before it was lost, soil movement was measured. The timing of loss coincided with a high water event (spring snow-melt flood). Most sensors were stationary for the majority of the time, with a few sudden movements. At the Pulmanki site, two soil scouts however also showed a prolonged movement pattern just after installation (Figure 5c–e), and at the palsa site, all installed soil scouts were continuously moving (Figure 4c–e).

At all sites, the measured temperature shows both the seasonal as well as the diurnal nature of the temperature fluctuations (Figures 3b–6b). When zooming in to a short time span, we can see that temperatures are slightly different between soil scouts (Figure 7). Comparing the temperature to the air temperature, we can see that peaks in the temperature occur later in the day than for air temperature and temperature amplitude is lower than that of the air temperature (Figure 7).

Soil moisture has a clear pattern, with spikes during strong precipitation events followed by a gradual lowering (Figures 3a–6a). In areas where there is a known influence of groundwater (Figure 5a, soil scouts 21164 and 21159; Figure 3a, soil scouts 20727/21153 and 20728/21152), the soil moisture shows higher values (Lotsari et al., 2020; H. Marttila, personal communication, 25/8/2022). At some locations, the soil moisture reacted much more strongly to precipitation events than at other locations (Figures 3a, 5a and 6a), and some soil scouts even did not see any rise in soil moisture. Soil moisture at some soil scout locations only reacted to some precipitation events. The change in soil moisture can thus be highly location dependent and might partly be influenced by installation depth (c.f. Hautala & Tiusanen, 2007).

### 4.2 | Interpretation of temperature lag

Differences between the air and soil temperature regime can be explained by the soil temperature lagging behind the air temperature (Hautala & Tiusanen, 2007), the amount of lag depending on the soil type and depth of the sensor. For example, soil scout 20739 measures a peak in temperature earlier than soil scout 20726. This lag can be quantified (Figure 8) and used to identify increases and decreases in the depth of the soil scouts, giving an additional metric to identify soil movement. Figure 8 for example shows that just after installation, the temperature phase at sensor 20714 decreased with respect to the other sensors at the field site, indicating that the soil scout was getting closer to the surface. At the same time, soil scout 20720 moved further away from the surface. These matched the movements seen from the digital accelerometer (c.f. Figure 5c,d). Between 15 June 2022 and 1 July 2022, the temperature phase at soil scout 20721 increased (Figure 8). No movement during this period was identified (c.f. Figure 5d,e), which insinuates that soil was deposited above the soil scout without moving the soil layer in which it was buried. Furthermore, soil scout 20717 shows a decrease in temperature phase shift (and thus depth) around 2 July, when it also moved (c.f. Figure 5c,d). Between 24 May 2022 and 29 May 2022, the data

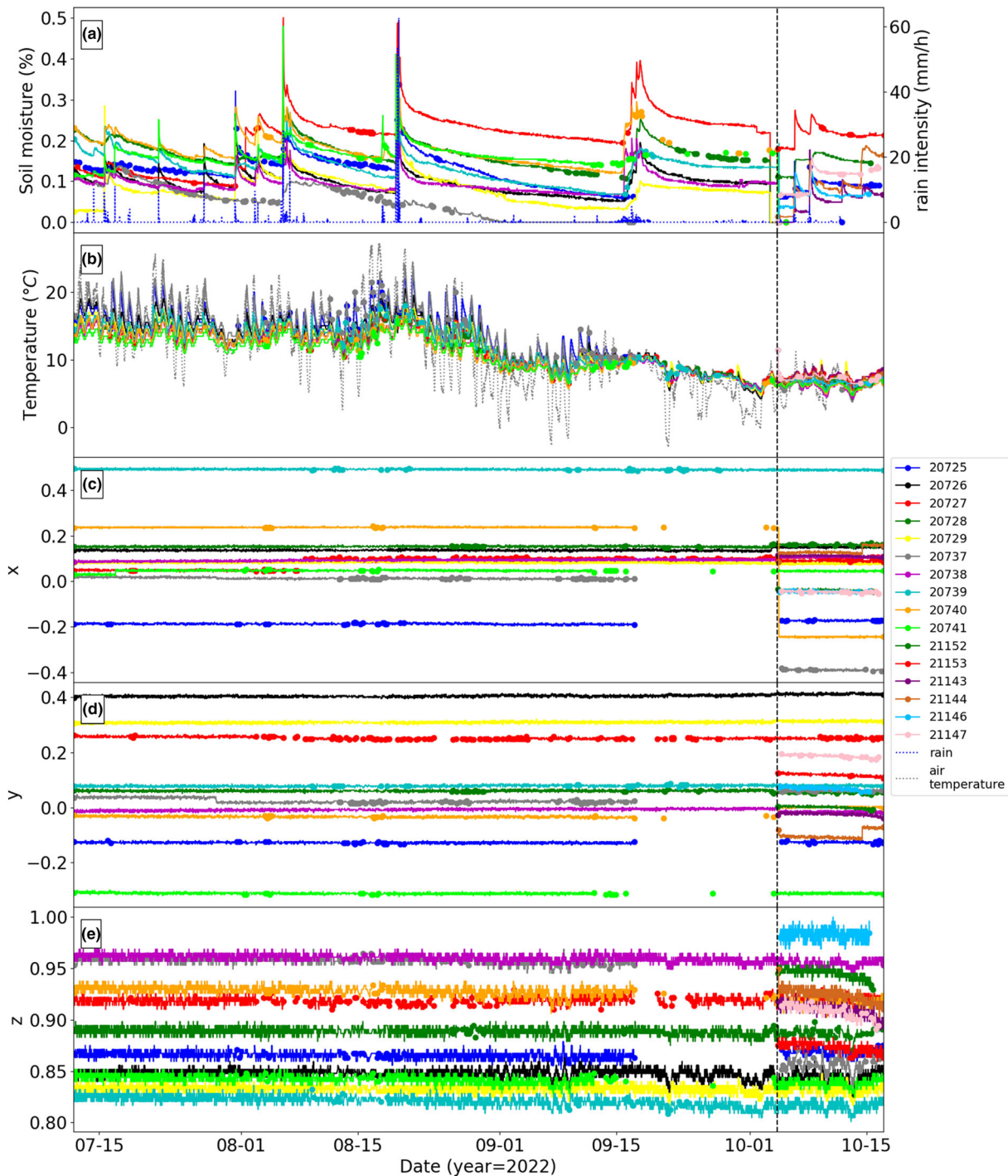


**FIGURE 3** Data obtained at the Oulanka field site. (a) Soil moisture and rain intensity from the Kiutaköngäs meteorological station (b) Measured soil temperature and air temperature from the Kiutaköngäs meteorological station. (c–e) Orientation of the  $x$ -,  $y$ - and  $z$ -axes. The vertical dashed line indicates the date that additional sensors were installed. Dots indicate the end or start of a data gap (defined as no received data points for at least 4 h). [Color figure can be viewed at [wileyonlinelibrary.com](https://onlinelibrary.wiley.com)]

packages of soil scout 20712 were not received, during which time its temperature phase decreased, indicating that some soil above it was eroded.

### 4.3 | Interpretation of data: correlation between soil movement and forcing parameters

The identified soil movements often occurred during or shortly after a precipitation event. At the Oulanka field site, soil scouts

20741 (16 July 2022) and 21144 (14 October 2022) showed this pattern. At the Vantaa field site, soil scout 20732 moved on 16 July 2022 also just after a precipitation event. However, this sensor was the only one at the site without a measured increase in soil moisture. Furthermore, during and after several days of rain around 15 September 2022, multiple soil scouts (21137, 21142, 20730, 20735 and 20736) moved. At all these locations, the soil moisture content increased, although only marginally at the location of scout 20735, which already had a high soil moisture content before the rain event began.

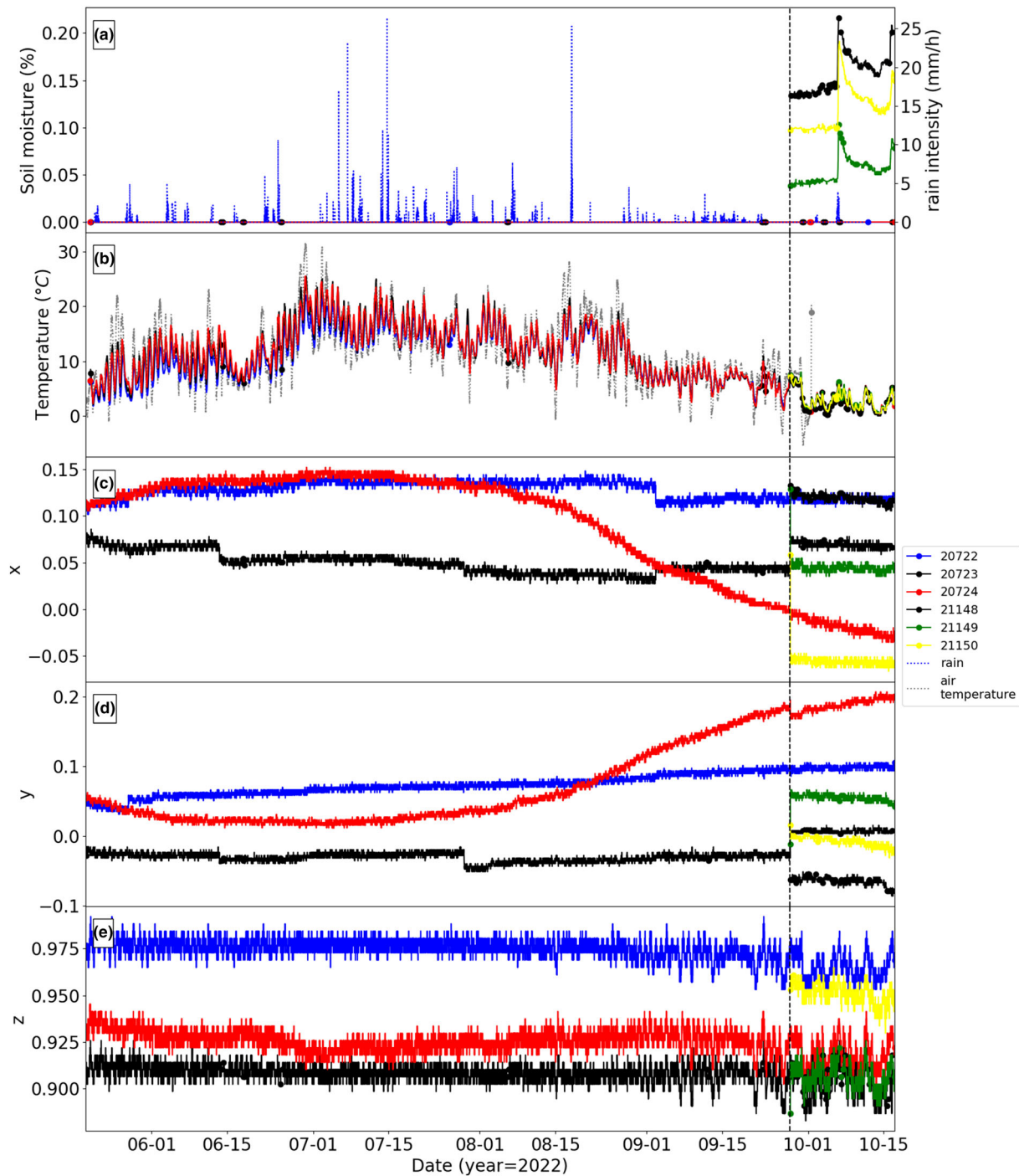


**FIGURE 4** Data obtained at the Pulmanki palsa site. (a) Soil moisture from the Nuorgam meteorological station. (b) Measured soil temperature and air temperature. (c–e) Orientation of the  $x$ -,  $y$ - and  $z$ -axes. The vertical dashed line indicates the date that additional sensors were installed. Dots indicate the end or start of a data gap (defined as no received data points for at least 4 h). [Color figure can be viewed at [wileyonlinelibrary.com](https://onlinelibrary.wiley.com)]

Because of the lack of soil moisture data at the Pulmanki field site, it is not possible to link soil movement events to increases in soil moisture. Based on meteorological data, it is still possible to deduce that some of the movements at the Pulmanki field site occurred during or shortly after (several hours) precipitation events (soil scouts 20719 and 20714 on 4 June 2022 and 26 July 2022, respectively). Furthermore, it was found that soil scout 20713 was lost during a high water event (26 May 2022); 1 day later, soil scout 20715, also installed close to the water level, moved, which can be attributed to the same high water event. Soil scout 20717 moved six times between 2 July and 3 August 2022, indicating that after the first movement, the soil remained unstable; the first movement occurred

after a small precipitation event (Figure 5a). Soil scout 20721 moved on 2 July 2022, likely after an aggradation event several days prior (Figure 8) left the bank less stable.

At the palsa site, continuous movement was identified, and the onset of this movement could therefore not be identified. The few sudden movements of soil scouts 20722 and 20723 are likely the result of the bank becoming unstable because of the continuous movement. At palsa mire, the melting of the permafrost core during the summer months causes the movement of the palsa mound and its edges to collapse into the thermokarst pond.

For several soil scouts, the reason or onset of movement remains unclear. So far, temperature seems to not yet have caused soil

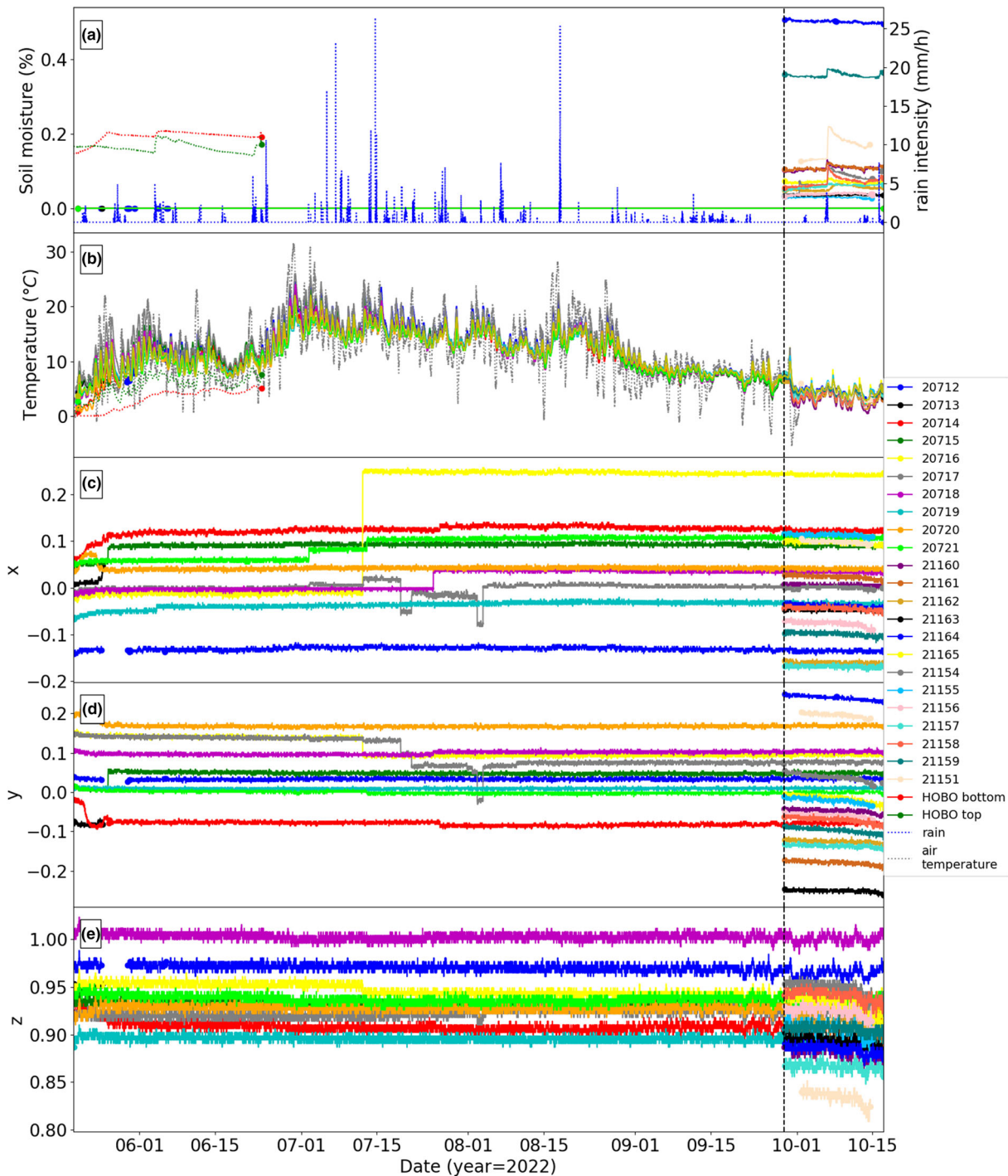


**FIGURE 5** Data obtained at the Pulmanki bank field site. (a) Soil moisture and rain intensity from the Nuorgam meteorological station. (b) Measured soil temperature and air temperature. (c–e) Orientation of the  $x$ -,  $y$ - and  $z$ -axes. The vertical dashed line indicates the date that additional sensors were installed. Dots indicate the end or start of a data gap (defined as no received data points for at least 4 h). [Color figure can be viewed at [wileyonlinelibrary.com](http://wileyonlinelibrary.com)]

movement to occur. This may change in winter when temperatures will drop and freezing and thawing of soil will occur. This is a topic of a later study, when there is longer term seasonal data available.

## 4.4 | Comparison with reference data sets

### 4.4.1 | DOD-based erosion locations

Figure 9 shows the DEM of difference for the period between 17 May 2022 and 26 September 2022 for the Pulmanki field site. Erosion is more prominent than aggradation at this bank site and is not

spread evenly over the area, with more erosion close to the top of the bank and close to the waterline. The erosion at the top of the bank may however be an artifact, because snow was still present during the drone flight on 17 May 2022, as such the elevation change at the top of the bank is likely caused by snow melt rather than bank erosion. Additionally, Figure 9 shows that at several locations, part of the bank collapsed, the material of which was deposited lower on the bank.

The soil sensor that was lost (20713) was in an area that was highly erosional in this period. Because of the moment that this soil scout was lost, and based on time-lapse camera data we know that this area has eroded on 25 May 2022. The other soil scouts are in

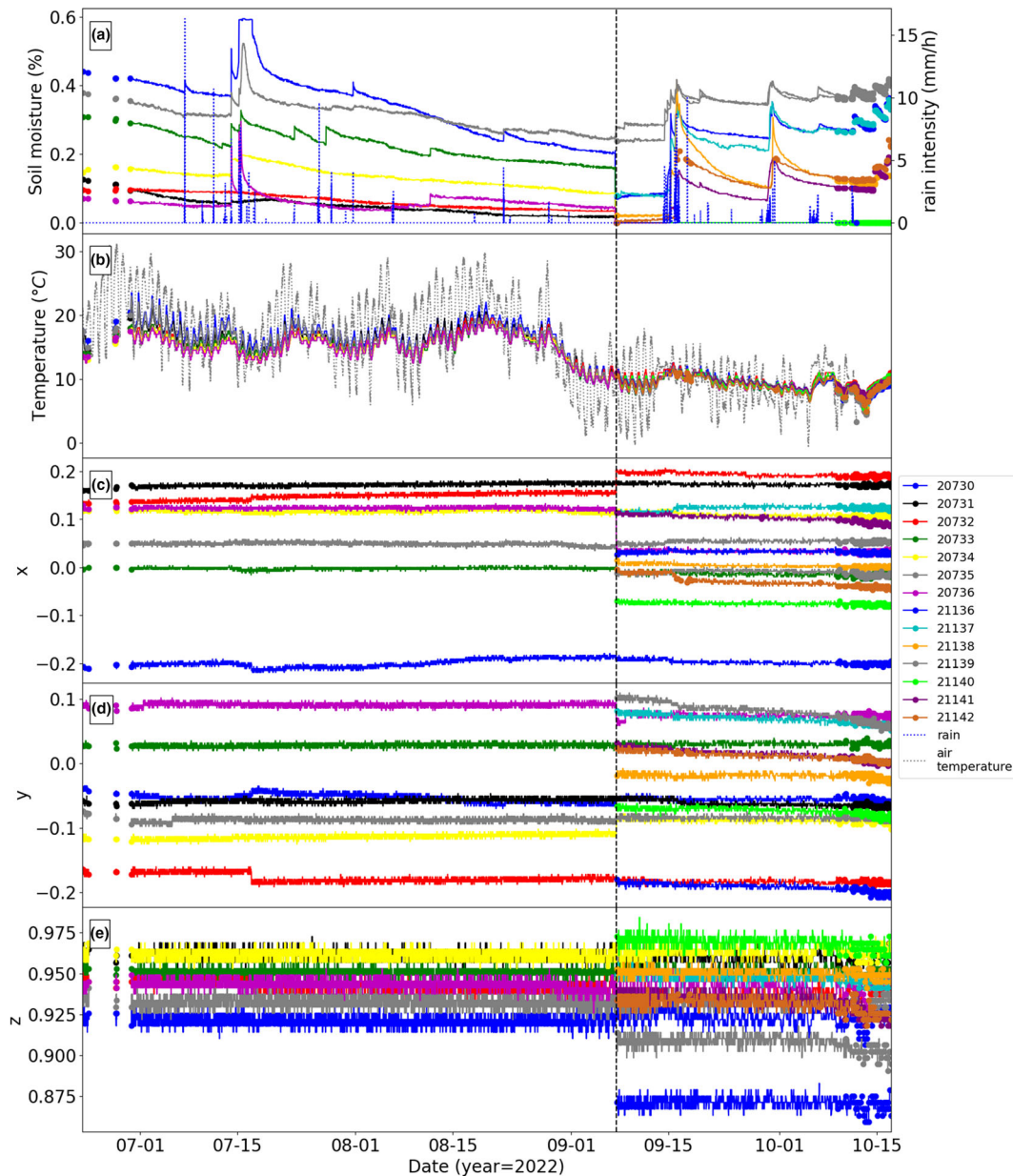


**FIGURE 6** Data obtained at the Vantaa field site. (a) Soil moisture from the Helsinki–Vantaa airport meteorological station. (b) Measured soil temperature and air temperature from the Helsinki–Vantaa airport meteorological station. (c–e) Movement around the x-, y- and z-axes. [Color figure can be viewed at [wileyonlinelibrary.com](https://onlinelibrary.wiley.com/terms-and-conditions)]

areas with much less elevational change (Figure 9). Most are in areas with minor erosion, but soil scouts 20718 and 20721 are in areas that might be slightly aggradational. The aggradation measured by the DEM of difference at the location of soil scout 20718 is not related to bank erosion, however. Soil scout 20718 is located under a tree overhanging the bank, and therefore, the DEM of difference at this location is measuring vegetation growth rather than aggradational processes. The aggradation at the location of soil scout 20721 is in agreement with the change in temperature phase (Figure 8). Some of the other soil scouts showed movement, even when located in areas where no elevation change was measured, indicating that even without a change in elevation, the bank is not stable and erosional processes are occurring. In contrast, soil scout 20714 did not show any movement, but at its location, erosion has occurred, showing that erosion does not necessarily cause soil movement at even modest depths.

#### 4.4.2 | Timing of the bank erosion based on time-lapse cameras

The imagery captured by the time-lapse cameras (Supporting Information) shows that erosion occurred at the location of sensor 20713 because of fluvial erosion during the rising stage of the spring flood. At the same time, the data packages from sensor 20712 were no longer received, which is likely caused by the water hampering the radio signal. Sensor 20717 was the sensor that had the most moving events; the cameras did not capture any soil movement for most of them. For the last two movement events (on 2 and 3 August), close to the location of the buried soil scout, an item resembling vegetation from on top of the bank fell onto the bank (2 August), which was later removed (3 August). These changes coincided with the measured soil movement and are the likely cause. The time-lapse cameras also show that just before the erosional event on 2 August reindeer were

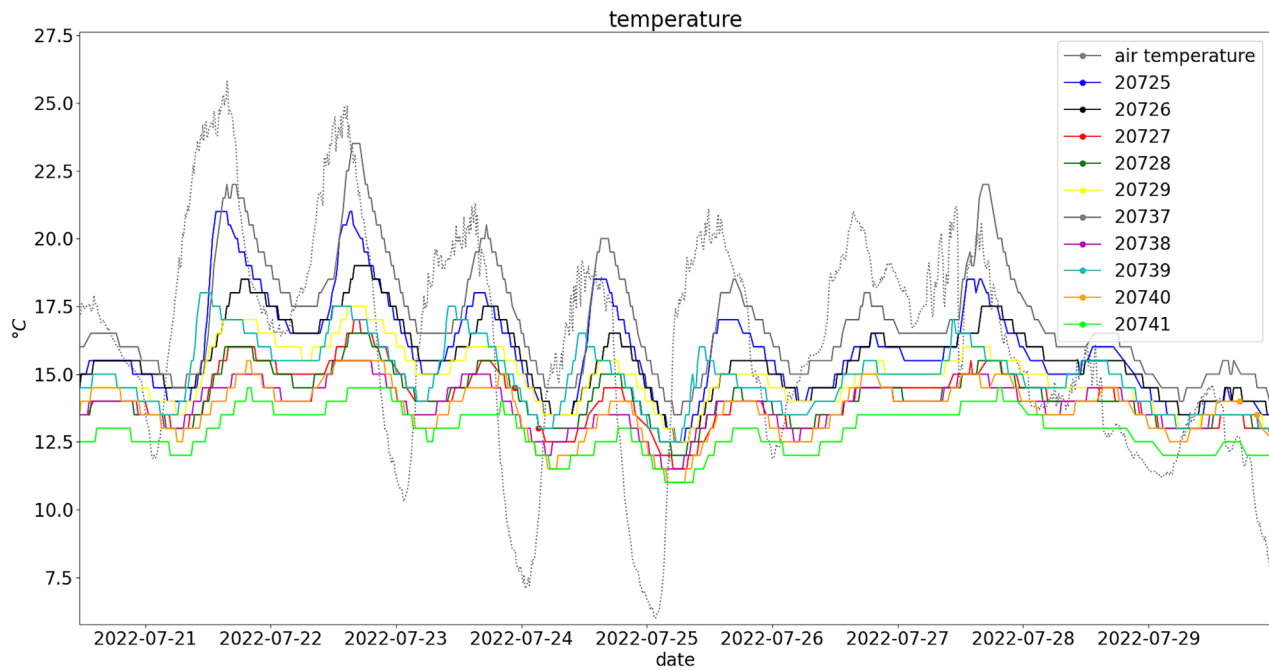


**FIGURE 7** Zoom in of the measured temperatures at the Oulanka field site. [Color figure can be viewed at [wileyonlinelibrary.com](https://onlinelibrary.wiley.com)]

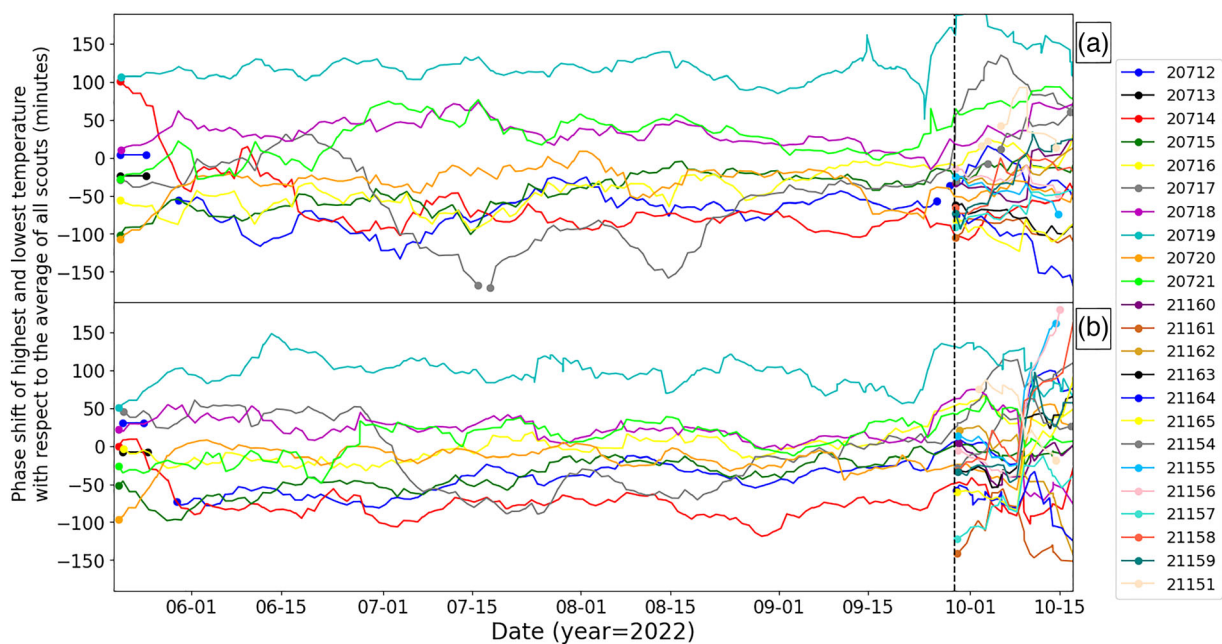


**FIGURE 8** The phase shift compared with the average phase shift of all installed soil scouts (in minutes) at the Pulmanki river bank field site. Averaged using a 9-day running average. (a) Phase shift of the daily maxima and (b) phase shift of the daily minima. [Color figure can be viewed at [wileyonlinelibrary.com](https://onlinelibrary.wiley.com)]

present on the bank (see Supporting Information). Finally, the movement of soil at the location of sensor 20716 could be seen around the time this sensor had a movement event (12 July).

#### 4.4.3 | Seismically detected bank erosion

During the 2-h-long window of time lapse-based bank failure activity starting on 2018-07-22 at 22:00 UTC, the seismic record depicts three distinct brief periods of seismic energy release (Figure 10) between frequencies of 5 to 60 Hz: 22:32, 22:42 and 23:08 UTC.

That frequency range and seismic power distribution are distinct from the other seismic patterns, during that period of interest (Figure 10b) and the data set as a whole (Figure 10a). The first of the three pulses consists of a single energy release, and the subsequent two each exhibit two slightly delayed energy release events (Figure 10c). Each of these events has a subtle onset but rapidly gains amplitude only to start decreasing slowly after reaching peak ground motion values. The in total five events last between 8 and 15 s. Apart from those brief pulses of activity, the sensor has also recorded a high-frequency (about 20–70 Hz) signal prolonged in time, starting around 22:00 UTC and ending around 23:15 UTC.

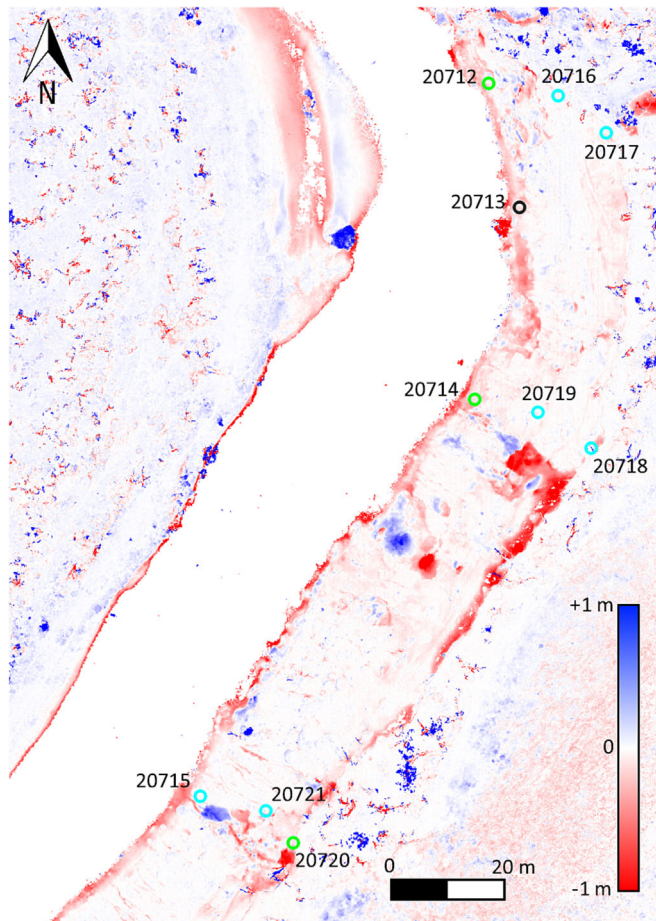


**FIGURE 9** DEM of difference for the Pulmanki field site showing the differences between 17 May and 26 September 2022; the markers show the sensors installed during the time period: black lost, cyan moved, green stable. [Color figure can be viewed at [wileyonlinelibrary.com](https://onlinelibrary.wiley.com)]

#### 4.4.4 | Interpretation of the seismic data

During the entire deployment period of 108 days (Figure 10a), the geophone has yielded a complete record at 0.005-s temporal resolution. During times when time-lapse imagery detected a bank failure (Figure 10b,d,e), some 35 m south-southwest of the geophone sensor, the seismic data can be used to provide a detailed anatomy of this process (Figure 10c). The cameras are capable of narrowing down the time of occurrence to a 2-h interval at best, that is if weather conditions were favourable. With the geophone, the onset time can be determined with sub-second resolution. Moreover, the entire evolution of a compound mass-wasting event can be quantified in terms of the number of single-release events, duration and relative seismic power, indicative of relative magnitude of an event. Thus, when combining these two survey techniques, one can get a detailed complementary picture of geomorphic activity important to a fluvial system.

Moreover, the seismometer was also sensitive to a likely trigger of the mass-wasting event itself. The 20- to 70-Hz signal during the time when the five granular flow events happened (Figure 10b) is typically attributed to rain, that is the multitude of drops pounding on the surface (c.f. Cook & Dietze, 2022; Dietze et al., 2017), which is coinciding with what the time-lapse pictures show (Figure 10d,e). Hence, geophones can shed detailed light onto the time-lagged, mechanistic coupling of drivers, triggers and events.

A next step forward would be to improve the geophysical station into a small network of sensors. This would allow to also seismically detect and locate bank failure events, to determine their released seismic energy (Le Roy et al., 2019) and inspect the effect of, for example sediment input into the stream for bedload transport activation thresholds.

#### 4.4.5 | HOBO soil and temperature logger comparison

In Figure 5b, the temperature measured using a HOBO temperature logger is shown. Two separate temperature loggers were attached to the HOBO logger buried at two different depths. The location of this logger was close to soil scout 20716. The HOBO logger shows lower temperatures and amplitudes in the temperature profile as soil scout 20716. This is because both temperature sensors were installed deeper than the soil scout. The same general pattern emerges, however.

Soil moisture cannot be directly compared with the soil moisture measurements of the soil scouts not only because of the fact that the first batch of soil scouts did not operate as required but also because of the fact that the HOBO-based soil moisture data were incomplete because of technical problems. The pattern in the soil moisture data of the HOBO logger (Figure 5a) is broadly similar to the patterns obtained with the soil scouts, for example sudden increases during precipitation events with a continuous decreasing soil moisture in between precipitation events.

## 5 | DISCUSSION

### 5.1 | Advantages of the soil scout approach

Soil scouts yield data with a high temporal resolution (every 20 min) for a long period of time (10 years). Temporal resolution of a monitoring technique used in bank erosion studies is typically around 1%–10% of the timescale of interest (Lawler, 1993), whereas for soil scouts, this is closer to 0.0004%, thus giving a much higher temporal resolution for the investigated period than is typical for other monitoring techniques (Table 1).

Data loss due to sensor loss is a realistic problem for measurement equipment that is present at the field site for extended periods of time such as erosion pins, PEEP sensors and sensors with dataloggers (e.g. Thorne, 1981). This might for instance happen because of vandalism, theft or high-water events. An advantage of the soil scout approach is that data are not lost upon sensor loss, because data are uploaded directly to the internet. For example, sensor 20713 was lost shortly after installation, but because data were sent just before the sensor was removed entirely, it was possible to deduce what had happened to the sensor and when. Of course, after sensor loss, subsequent erosion at this location could not be measured, until a new sensor was installed.

The automatic uploading of data to the cloud storage also limits the number of field visits that are required. This makes the approach useful in places that are far away or are difficult to reach, especially compared with approaches that require an investigator to be present

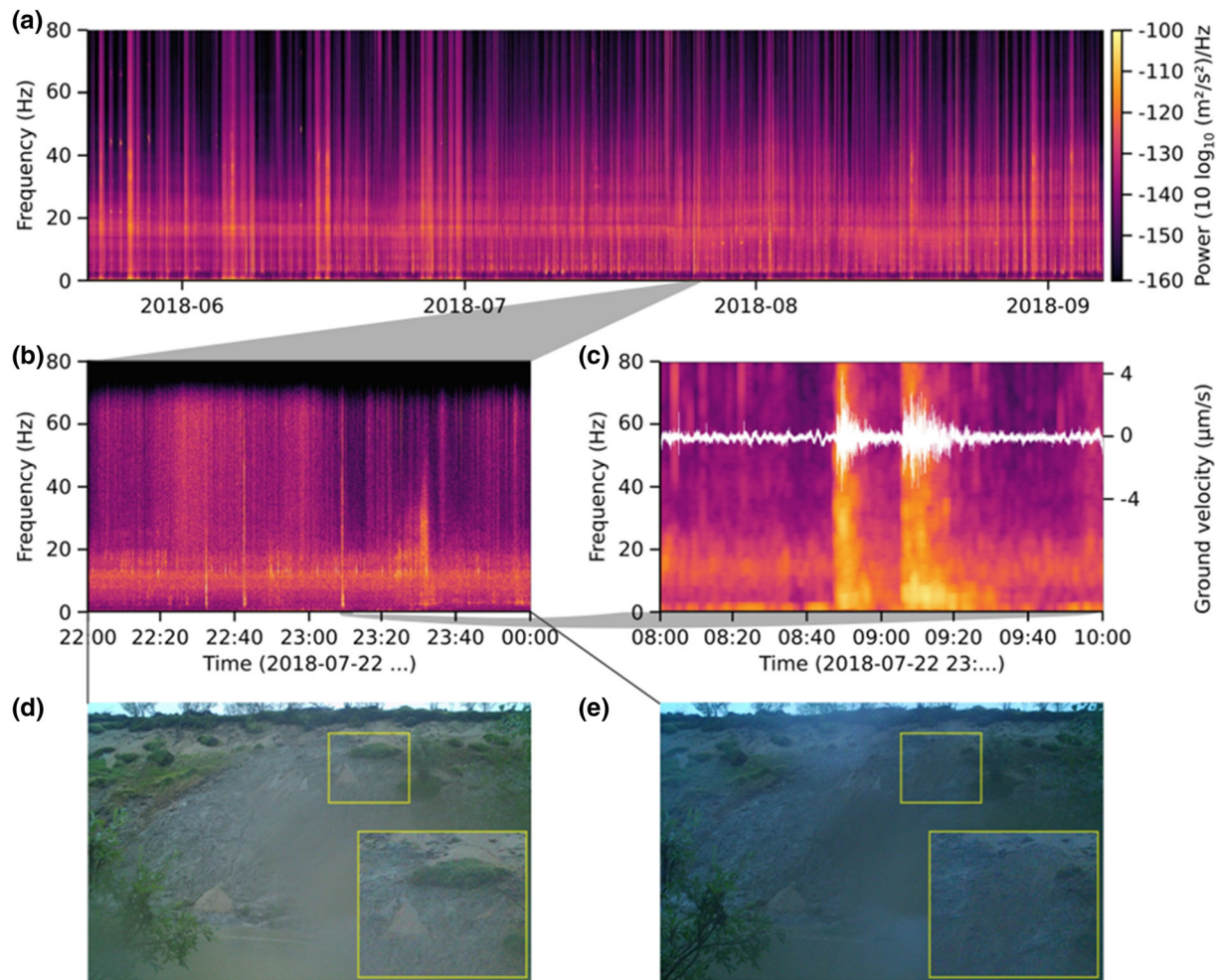


**FIGURE 10** Seismic and photographic evidence of bank activity. (a) Seismic spectrogram of the full deployment time showing diurnal pattern of background activity (vertical patterns) and continuous river turbulence signal (horizontal orange band at 10–20 Hz). (b) Zoom to potential bank activity period as indicated by time-lapse imagery with three phases of pulsed hillslope mass wasting signatures (22:32 UTC, 22:42 UTC and 23:08 UTC). (c) Detailed anatomy of the third activity pulse with seismogram (white overlay). (d) Time-lapse picture before (22:00) and (e) after (00:00) the bank failure event has happened. Note: poor image quality due to night time hours and strong precipitation. [Color figure can be viewed at [wileyonlinelibrary.com](http://wileyonlinelibrary.com)]

to take the measurement (e.g. erosion pins, comparison of DTMs, repeated cross-profiling, marked pebbles, lateral flow collection flumes, manual measurements and markers: c.f. Table 1; Barker et al., 1997; Bernatchez & Dubois, 2008; Duró et al., 2018; Fox et al., 2007; Hamshaw et al., 2019; Kaczmarek et al., 2021; Midgley et al., 2013; Prosser et al., 2000; Thoma et al., 2005; Thorne, 1978; Veihe et al., 2011; Wilson et al., 2007; Yumoto et al., 2006) or ones that require regular downloading of the data (e.g. PEEP sensors, tensiometers-piezometers and sensors with dataloggers: c.f. Table 1; Casagli et al., 1999; Lawler, 1993, 2005; Rinaldi et al., 2004). However, note that the base station must be in an area where there is mobile phone connection, in order to upload the data to the cloud. This may limit the applicability of the approach in some remote areas. However, mobile phone networks are improving worldwide, and we were already able to utilize the approach in a remote area (Pulmanki field site), by placing the base station on a hill where the mobile phone connection is sufficient. If mobile phone connection is not available close enough to the field site, it is also possible to place the base station further away in an area with mobile phone connection and place one or more echo stations in between, so as to close the gap between the base and the sensors.

The addition of the digital accelerometer within soil scouts allowed for the monitoring of soil movement. The temporal resolution of the sensor system is high enough that the timing of soil movement can be assessed as well, and it was possible to discern between sudden and continuous movement. This makes the used approach unique, as few approaches can make this distinction (out of all approaches in Table 1, only the PEEP sensors). Furthermore, the fact that one sensor measures both the soil movement as well as the important parameters for bank erosion allows for the identification of the cause of erosion for individual events. So far, no approach is available with this capability.

## 5.2 | Disadvantages and limitations of the soil scout approach

At the Pulmanki and Vantaa sites, all installed sensors connected without fail. However, at the Oulanka field site, connection problems were more frequent. The vegetated state of the Oulanka field site partly contributed to this; the vegetation can block the radio signal that transfers the data from the soil scout to the base or echo station.

Furthermore, the topography of the region, including the direction of the slope in which the sensor is installed with respect to the echo or base, can have a major impact on the chance that a data package can be received successfully. This is due to the radio signal refracting at the soil–air interface (Tiusanen, 2005, 2013). A slope facing the echo or base station will have better connections, whereas a slope facing away from an echo or base station will greatly reduce the chance of successful transmission. At both the Pulmanki and Vantaa sites, the base station is on the opposite side of the river, ensuring that the slope is always optimally oriented, whereas at the Oulanka field site, the slope orientation is more variable. We therefore recommend that in future studies into bank erosion where soil scouts are used, the base or echo station is to be installed on the opposite side of the river, to ensure optimal transmission of the data packages. Finally, the distance to the water can be of influence. Soil scouts can be installed under the water level, but the radio signal range will be reduced. Because of this, data packages from soil scout 20717 did not arrive for several days during a high water event just after installation. From Figure 8, we can infer that this was caused by the high water and not by additional soil piling on top of the soil scout, because erosion occurred at this location, not deposition. Care should thus be taken with regard to the location and positioning of the sensors, which adds a layer of complexity, which other measurement approaches do not have.

Likewise, the location of installation influenced the ease of installation. Although the installation was generally easy and no heavy equipment was required, installation speed varied and increased with experience. In good conditions, less than 10 min per soil scout was required for installation. Vegetation, type of subsoil and/or steepness of the bank could complicate installation.

The sensors are installed into the river bank in order to measure erosion. As a result, when erosion occurs, they move. After some time, the exact location of the sensor may become unclear, which could hinder the analysis of the data. When retrieving the additional ‘standard’ soil scouts, some had moved from the documented location. Especially for long-term studies in very active sites, this could present a challenge. With exception of marked pebbles, of which also the location may become unknown if they cannot be found again, no other measurement approaches have the problem that the measurement device’s location could become unknown. In a similar fashion, the soil movement due to erosion may reorient the soil scout or bury it deeper into the bank, both of which could potentially cause the radio signal the soil scout uses to send its data packages to the base station to not be strong enough, leading to potential loss of data. This may be uncommon however, because movement around the z-axis (Figure 2a) is rare (Figures 3e–6e); movement around the z-axis would most quickly lead to a new orientation of the radio signal.

Although the soil scouts can directly measure the timing of soil movement, their ability to measure the amount of erosion is limited. However, erosion and sedimentation can, at least theoretically, be inferred from the temperature phase analysis, although more research is needed for this. Regardless, this will only yield information on the amount of bank-level change at a point location. Therefore, especially when the quantity of bank material supplied to the stream is of interest, other approaches such as erosion pins, PEEP sensors or comparison of DTMs may be more suitable.

Soil moisture and temperature often change with depth. Soil movement through creep is also likely to change with depth, for example the top layer of soil may move, whereas the underlying layers remain stationary. Soil scouts are only able to obtain data at the depth they are installed. Although soil scouts can be buried at different depths, burying multiple sensors above one another is not possible since radio signals can interfere, leading to one of the sensors not connecting. Soil scouts may thus be ineffective when the vertical profile of erosional parameters in a river bank has to be monitored. However, soil scouts can be buried at different depths several decimetres apart from one another if this information is required. If the variation over depth at one specific location is required, the HOBO loggers as used in this work or tensiometer-piezometers may be a more effective alternative (c.f. Table 1; Casagli et al., 1999; Rinaldi et al., 2004; Yumoto et al., 2006). Note, however, that no other approach from Table 1 is able to monitor subsurface soil movement.

Finally, although soil scouts impact the bank minimally, they do still influence the bank. These are concentrated around the time of installation. For example, some soil scouts show small movements directly after installation, which do not follow the normal movement pattern at the field site (e.g. Figure 5c,d, soil scouts 20714 and 20720). These movements are likely the result of the soil above the soil scout compacting, slightly moving the soil scout. Another example can be found in the soil moisture. At the Vantaa field site, it was not possible to retrieve one of the ‘standard’ soil scouts used to measure the soil moisture (Figure 6a, indicated with soil scout 20735). When a new soil scout was placed close to it (soil scout 21139), it initially measured a lower soil moisture content. After a precipitation event, the soil moisture measured by both soil scouts was virtually identical (Figure 6a). The soil moisture in the area where a hole was dug is thus affected until the first precipitation event after installation.

The soil scouts minimally disturb the bank itself. The small size, lack of wire or rod that extends to the bank surface or into the bank and no requirement to revisit installed sensors all contribute to the minimal disturbance compared with other approaches (such as erosion pins, PEEP sensors, repeated cross-profiling, marked pebbles, sensors with dataloggers and markers; also see Thorne, 1981; Veihe et al., 2011). The bank is only disturbed during the sensor installation by the walking and digging by the investigators. However, there are also some approaches, such as comparison of DTMs, that do not disturb the measured bank at all.

### 5.3 | Outlook

The used soil sensors are unique in supplying high-frequency soil moisture and temperature data at the same locations where soil movement is monitored. Additionally, they can be placed over a large area. However, they take point measurements; thus, even though the temporal resolution is high and the spatial and temporal extent are large, the spatial resolution is low. Combining the soil scouts with approaches with a high spatial resolution, such as spatially continuous data sets, could therefore be especially fruitful. Both geophones and the comparison of DEMs could fill this role for erosion data. For example, the DoD approach has a high spatial resolution and can give detailed information on the location and extent of geographical

change (Barker et al., 1997; Brasington et al., 2000; Duró et al., 2018; Hamshaw et al., 2019; Leyland et al., 2017; Sekely et al., 2002; Thoma et al., 2005). It however lacks in temporal resolution. This can be further complemented by geophones, which are also able to estimate the location of geographical change (if at least three stations are used), while also improving the temporal frequency even further (Cook & Dietze, 2022; Dietze et al., 2020). Similarly, time-lapse imagery can be used to infer the spatial extent of movement identified by soil scouts.

For temperature and soil moisture, only few approaches are available to directly measure these at high spatial resolutions (fibre optic cables and electrical resistivity tomography; Banks et al., 2022; Jodry et al., 2019). Obtaining high spatial data on temperature or soil moisture might require modelling that has also seen successes (e.g. Kimiaghdam et al., 2015; Rinaldi et al., 2004), although the models do often need detailed information about the subsoil or point measurements. Further research into how the soil scout data can be used to model banks may prove particularly useful and would also bring us closer to developing digital twins of river systems. Ultimately, the combination of approaches will always depend on the research or monitoring goal, but complementing the soil scout measurements with other measurement approaches has great potential.

It is possible to obtain more information from the soil scout data itself. Using the temperature phase to identify the depth of the soil scouts and from that infer erosion and aggradation of the soil above the sensor shows potential. However, currently, exact changes in depth cannot be identified, and the meteorological day-to-day changes make it difficult to identify small changes in temperature phase. More research is needed to identify the effect of soil type, bank angle and bank orientation on the temperature profile in river banks and accuracy of the methodology. This could ultimately be used to quantify erosion and deposition at high frequencies at the point locations the soil scouts are buried. Nevertheless, Figure 8 shows that it is already possible to identify increases in depth (suggesting deposition or movement) and decreases in depth (suggesting erosion or movement). Comparing these data with the movement data can show if soil above the soil scout moved without moving the soil layer in which the soil scout is buried.

## 6 | CONCLUSIONS

In this work, novel sensors (soil scouts) developed for the agricultural industry were tested for application in the monitoring of riverbank erosion. The soil scout approach has several unique advantages over existing approaches for the measuring and monitoring of river banks. They yield very high-resolution data on both soil movement as well as the forcing parameters at the same location for an extended period of time. This allows the timing of soil erosion to be identified. Furthermore, very limited attention by the investigator is required once the system has been installed because data are automatically uploaded to a cloud storage. This also makes the approach suitable for long-term monitoring.

However, the soil scout approach to measuring bank erosion is not perfect. Measuring the parameters over a depth profile is not possible. The movement of the bank in which the sensors are installed may also make the exact location of measurements unclear after the

sensor has identified movement several times. Monitoring river bank erosion using the soil scout approach may also yield an insufficient spatial resolution.

Overall, soil scouts have several unique advantages and disadvantages and can be a good tool for the monitoring of river bank erosion and topographical changes. Combining soil scouts with other monitoring approaches that have different strengths, such as a high spatial resolution, could enhance river bank modelling and lead to new insights.

## ACKNOWLEDGEMENTS

We would like to thank MSc Tuure Takala and MSc Juha-Matti Välimäki from Aalto University and numerous other field assistants and collaborators from the University of Eastern Finland and the University of Turku, who have helped with the seasonal checks of the time-lapse cameras, geophone and HOBO sensors. We also thank Soil Scout company for helping with installation and solving technical problems with the sensors. We also thank the Oulanka research station crew for their assistance in 2022 during the measurements and installations at the Oulanka site and the landowners of the sites for permission for sensor installation. Finally, we want to extend our gratitude to the two anonymous reviewers whose comments improved the work.

## CONFLICT OF INTEREST STATEMENT

A conflict of interest was not perceived.

## DATA AVAILABILITY STATEMENT

Data access can be granted on a case-by-case basis by contacting the corresponding author.

## ORCID

Erik van Rooijen  <https://orcid.org/0000-0003-3701-6682>

Eliisa Lotsari  <https://orcid.org/0000-0002-0120-8722>

## REFERENCES

- Banks, E.W., Morgan, L.K., Sai Louie, A.J., Dempsey, D. & Wilson, S.R. (2022) Active distributed temperature sensing to assess surface water-groundwater interaction and river loss in braided river systems. *Journal of Hydrology*, 615, 128667. Available from: <https://doi.org/10.1016/j.jhydrol.2022.128667>
- Barker, R., Dixon, L. & Hooke, J. (1997) Use of terrestrial photogrammetry for monitoring and measuring bank erosion. *Earth Surface Processes and Landforms*, 22(13), 1217–1227. Available from: [https://doi.org/10.1002/\(SICI\)1096-9837\(199724\)22:13<1217::AID-ESP819>3.0.CO;2-U](https://doi.org/10.1002/(SICI)1096-9837(199724)22:13<1217::AID-ESP819>3.0.CO;2-U)
- Bernatchez, P. & Dubois, J.M.M. (2008) Seasonal quantification of coastal processes and cliff erosion on fine sediment shorelines in a cold temperate climate, north shore of the St. Lawrence maritime estuary, Québec. *Journal of Coastal Research*, 1, 169–180. Available from: <https://doi.org/10.2112/04-0419.1>
- Best, J. (2019) Anthropogenic stresses on the world's big rivers. *Nature Geoscience*, 12(1), 7–21. Available from: <https://doi.org/10.1038/s41561-018-0262-x>
- Bouchard, F., MacDonald, L.A., Turner, K.W., Thienpont, J.R., Medeiros, A.S., Biskaborn, B.K. et al. (2016) Paleolimnology of thermokarst lakes: a window into permafrost landscape evolution. *Arctic Science*, 3(2), 91–117. Available from: <https://doi.org/10.1139/as-2016-0022>
- Brasington, J., Rumsby, B.T. & McVey, R.A. (2000) Monitoring and modelling morphological change in a braided gravel-bed river using high

- resolution GPS-based survey. *Earth surface processes and landforms: the journal of the British Geomorphological Research Group*, 25(9), 973–990. Available from: [https://doi.org/10.1002/1096-9837\(200008\)25:9<973::AID-ESP111>3.0.CO;2-Y](https://doi.org/10.1002/1096-9837(200008)25:9<973::AID-ESP111>3.0.CO;2-Y)
- Casagli, N., Rinaldi, M., Gargini, A. & Curini, A. (1999) Pore water pressure and streambank stability: results from a monitoring site on the Sieve River, Italy. *Earth Surface Processes and Landforms: the Journal of the British Geomorphological Research Group*, 24(12), 1095–1114. Available from: [https://doi.org/10.1002/\(SICI\)1096-9837\(199911\)24:12<1095::AID-ESP37>3.0.CO;2-F](https://doi.org/10.1002/(SICI)1096-9837(199911)24:12<1095::AID-ESP37>3.0.CO;2-F)
- Chassiot, L., Lajeunesse, P. & Bernier, J.F. (2020) Riverbank erosion in cold environments: review and outlook. *Earth-Science Reviews*, 207, 103231. Available from: <https://doi.org/10.1016/j.earscirev.2020.103231>
- Cook, K.L. & Dietze, M. (2022) Seismic advances in process geomorphology. *Annual Review of Earth and Planetary Sciences*, 50(1), 183–204. Available from: <https://doi.org/10.1146/annurev-earth-032320-085133>
- Couper, P.R. & Maddock, I.P. (2001) Subaerial river bank erosion processes and their interaction with other bank erosion mechanisms on the River Arrow, Warwickshire, UK. *Earth Surface Processes and Landforms: the Journal of the British Geomorphological Research Group*, 26(6), 631–646. Available from: <https://doi.org/10.1002/esp.212>
- Darby, S.E., Rinaldi, M. & Dapporto, S. (2007) Coupled simulations of fluvial erosion and mass wasting for cohesive river banks. *Journal of Geophysical Research - Earth Surface*, 112(F3), F03022. Available from: <https://doi.org/10.1029/2006JF000722>
- Dietze, M. (2018) The R package “eseis”—a software toolbox for environmental seismology. *Earth Surface Dynamics*, 6(3), 669–686. Available from: <https://doi.org/10.5194/esurf-6-669-2018>
- Dietze, M., Losee, J., Polvi, L. & Palm, D. (2020) A seismic monitoring approach to detect and quantify river sediment mobilization by steel-head redd-building activity. *Earth Surface Processes and Landforms*, 45(12), 2840–2849. Available from: <https://doi.org/10.1002/esp.4933>
- Dietze, M., Mohadjer, S., Turowski, J.M., Ehlers, T.A. & Hovius, N. (2017) Seismic monitoring of small alpine rockfalls—validity, precision and limitations. *Earth Surface Dynamics*, 5(4), 653–668. Available from: <https://doi.org/10.5194/esurf-5-653-2017>
- Duró, G., Crosato, A., Kleinhans, M.G. & Uijttewaal, W.S. (2018) Bank erosion processes measured with UAV-SfM along complex banklines of a straight mid-sized river reach. *Earth Surface Dynamics*, 6(4), 933–953. Available from: <https://doi.org/10.5194/esurf-6-933-2018>
- Feng, Z.Y., Hsu, C.M. & Chen, S.H. (2019) Discussion on the characteristics of seismic signals due to riverbank landslides from laboratory tests. *Water*, 12(1), 83. Available from: <https://doi.org/10.3390/w12010083>
- Fox, G.A., Wilson, G.V., Simon, A., Langendoen, E.J., Akay, O. & Fuchs, J.W. (2007) Measuring streambank erosion due to ground water seepage: correlation to bank pore water pressure, precipitation and stream stage. *Earth Surface Processes and Landforms: the Journal of the British Geomorphological Research Group*, 32(10), 1558–1573. Available from: <https://doi.org/10.1002/esp.1490>
- Frauenfeld, O.W., Zhang, T. & McCreight, J.L. (2007) Northern hemisphere freezing/thawing index variations over the twentieth century. *International Journal of Climatology: a Journal of the Royal Meteorological Society*, 27(1), 47–63. Available from: <https://doi.org/10.1002/joc.1372>
- Green, T.R., Beavis, S.G., Dietrich, C.R. & Jakeman, A.J. (1999) Relating stream-bank erosion to in-stream transport of suspended sediment. *Hydrological Processes*, 13(5), 777–787. Available from: [https://doi.org/10.1002/\(SICI\)1099-1085\(19990415\)13:5<777::AID-HYP780>3.0.CO;2-P](https://doi.org/10.1002/(SICI)1099-1085(19990415)13:5<777::AID-HYP780>3.0.CO;2-P)
- Hamshaw, S.D., Engel, T., Rizzo, D.M., O'Neil-Dunne, J. & Dewoolkar, M.M. (2019) Application of unmanned aircraft system (UAS) for monitoring bank erosion along river corridors. *Geomatics, Natural Hazards and Risk*, 10(1), 1285–1305. Available from: <https://doi.org/10.1080/19475705.2019.1571533>
- Hautala, M. & Tiusanen, J. (2007) Depth determination of a wireless underground Soil Scout. *Precision Agriculture*, 7, 333–339. Available from: <https://doi.org/10.3920/978-90-8686-603-8>
- Hibert, C., Mangeney, A., Grandjean, G. & Shapiro, N.M. (2011) Slope instabilities in Dolomieu crater, Réunion Island: from seismic signals to rockfall characteristics. *Journal of Geophysical Research - Earth Surface*, 116(F4), F04032. Available from: <https://doi.org/10.1029/2011JF002038>
- Hutton, D. & Haque, C.E. (2004) Human vulnerability, dislocation and resettlement: adaptation processes of river-bank erosion-induced displaces in Bangladesh. *Disasters*, 28(1), 41–62. Available from: <https://doi.org/10.1111/j.0361-3666.2004.00242.x>
- IPCC. (2022) In: Pörtner, H.-O., Roberts, D.C., Tignor, M., Poloczanska, E.S., Mintenbeck, K., Alegria, A., et al. (Eds.) *Climate change 2022: impacts, adaptation, and vulnerability. Contribution of working group II to the sixth assessment report of the intergovernmental panel on climate change*. Cambridge, UK and New York, NY, USA: Cambridge University Press. Cambridge University Press, p. 3056. Available from: <https://doi.org/10.1017/9781009325844>
- Jodry, C., Lopes, S.P., Fargier, Y., Sanchez, M. & Côte, P. (2019) 2D-ERT monitoring of soil moisture seasonal behaviour in a river levee: a case study. *Journal of Applied Geophysics*, 167, 140–151. Available from: <https://doi.org/10.1016/j.jappgeo.2019.05.008>
- Kaczmarek, H., Bartczak, A., Tyszkowski, S., Badocha, M. & Krzemiński, M. (2021) The impact of freeze-thaw processes on a cliff recession rate in the face of temperate zone climate change. *Catena*, 202, 105259. Available from: <https://doi.org/10.1016/j.catena.2021.105259>
- Kimiaghalam, N., Goharrokhi, M., Clark, S.P. & Ahmari, H. (2015) A comprehensive fluvial geomorphology study of riverbank erosion on the Red River in Winnipeg, Manitoba, Canada. *Journal of Hydrology*, 529, 1488–1498. Available from: <https://doi.org/10.1016/j.jhydrol.2015.08.033>
- Kronvang, B., Grant, R. & Laubel, A.L. (1997) Sediment and phosphorus export from a lowland catchment: quantification of sources. *Water, Air, and Soil Pollution*, 99(1), 465–476. Available from: <https://doi.org/10.1007/BF02406886>
- Langendoen, E.J. & Simon, A. (2008) Modeling the evolution of incised streams. II: streambank erosion. *Journal of Hydraulic Engineering*, 134(7), 905–915. Available from: [https://doi.org/10.1061/\(ASCE\)0733-9429\(2008\)134:7\(905](https://doi.org/10.1061/(ASCE)0733-9429(2008)134:7(905)
- Lawler, D.M. & Leeks, G.J.L. (1992) River bank erosion events on the Upper Severn detected by the photo-electronic erosion pin (PEEP) system. *Erosion and Sediment Transport Monitoring Programmes in River Basins*, 200, 95–105.
- Lawler, D.M. (1986) River bank erosion and the influence of frost: a statistical examination. *Transactions of the Institute of British Geographers*, 11(2), 227–242. Available from: <https://doi.org/10.2307/622008>
- Lawler, D.M. (1993) The measurement of river bank erosion and lateral channel change: a review. *Earth Surface Processes and Landforms*, 18(9), 777–821. Available from: <https://doi.org/10.1002/esp.3290180905>
- Lawler, D.M. (2005) The importance of high-resolution monitoring in erosion and deposition dynamics studies: examples from estuarine and fluvial systems. *Geomorphology*, 64(1–2), 1–23. Available from: <https://doi.org/10.1016/j.geomorph.2004.04.005>
- Lawler, D.M. (2008) Advances in the continuous monitoring of erosion and deposition dynamics: developments and applications of the new PEEP-3T system. *Geomorphology*, 93(1–2), 17–39. Available from: <https://doi.org/10.1016/j.geomorph.2006.12.016>
- Le Roy, G., Helmstetter, A., Amiran, D., Guyoton, F. & Le Roux-Mallouf, R. (2019) Seismic analysis of the detachment and impact phases of a rockfall and application for estimating rockfall volume and free-fall height. *Journal of Geophysical Research - Earth Surface*, 124(11), 2602–2622. Available from: <https://doi.org/10.1029/2019JF004999>
- Lekshmi, S.U.S., Singh, D.N. & Baghini, M.S. (2014) A critical review of soil moisture measurement. *Measurement*, 54, 92–105. Available from: <https://doi.org/10.1016/j.measurement.2014.04.007>

- Leyland, J., Hackney, C.R., Darby, S.E., Parsons, D.R., Best, J.L., Nicholas, A.P. et al. (2017) Extreme flood-driven fluvial bank erosion and sediment loads: direct process measurements using integrated mobile laser scanning (MLS) and hydro-acoustic techniques. *Earth Surface Processes and Landforms*, 42(2), 334–346. Available from: <https://doi.org/10.1002/esp.4078>
- Lotsari, E., Hackney, C., Salmela, J., Kasvi, E., Kemp, J., Alho, P. et al. (2020) Sub-arctic river bank dynamics and driving processes during the open-channel flow period. *Earth Surface Processes and Landforms*, 45(5), 1198–1216. Available from: <https://doi.org/10.1002/esp.4796>
- Lotsari, E., Lind, L. & Kämäri, M. (2019) Impacts of hydro-climatically varying years on ice growth and decay in a subarctic river. *Water*, 11(10), 2058. Available from: <https://doi.org/10.3390/w11102058>
- Lotsari, E., Vaaja, M., Flener, C., Kaartinen, H., Kukko, A., Kasvi, E. et al. (2014) Annual bank and point bar morphodynamics of a meandering river determined by high-accuracy multitemporal laser scanning and flow data. *Water Resources Research*, 50(7), 5532–5559. Available from: <https://doi.org/10.1002/2013WR014106>
- Matsuoka, N. (1994) Continuous recording of frost heave and creep on a Japanese alpine slope. *Arctic and Alpine Research*, 26(3), 245–254. Available from: <https://doi.org/10.2307/1551937>
- Matsuoka, N. (1996) Soil moisture variability in relation to diurnal frost heaving on Japanese high mountain slopes. *Permafrost and Periglacial Processes*, 7(2), 139–151. Available from: [https://doi.org/10.1002/\(SICI\)1099-1530\(199604\)7:2<139::AID-PPP214>3.0.CO;2-V](https://doi.org/10.1002/(SICI)1099-1530(199604)7:2<139::AID-PPP214>3.0.CO;2-V)
- Matsuoka, N. (2001) Solifluction rates, processes and landforms: a global review. *Earth-Science Reviews*, 55(1–2), 107–134. Available from: [https://doi.org/10.1016/S0012-8252\(01\)00057-5](https://doi.org/10.1016/S0012-8252(01)00057-5)
- Matsuoka, N. (2005) Temporal and spatial variations in periglacial soil movements on alpine crest slopes. *Earth Surface Processes and Landforms: the Journal of the British Geomorphological Research Group*, 30(1), 41–58. Available from: <https://doi.org/10.1002/esp.1125>
- Meyer, A.M., Klein, C., Fünfroeken, E., Kautenburger, R. & Beck, H.P. (2019) Real-time monitoring of water quality to identify pollution pathways in small and middle scale rivers. *Science of the Total Environment*, 651(Pt 2), 2323–2333. Available from: <https://doi.org/10.1016/j.scitotenv.2018.10.069>
- Midgley, T.L., Fox, G.A., Wilson, G.V., Heeren, D.M., Langendoen, E.J. & Simon, A. (2013) Seepage-induced streambank erosion and instability: in situ constant-head experiments. *Journal of Hydrologic Engineering*, 18(10), 1200–1210. Available from: [https://doi.org/10.1061/\(ASCE\)1084-0699\(2013\)18:10\(1200\)](https://doi.org/10.1061/(ASCE)1084-0699(2013)18:10(1200))
- Moteki, D., Murai, T., Hoshino, T., Yasuda, H., Muramatsu, S. & Hayasaka, K. (2022) Capture method for digital twin of formation processes of sand bars. *Physics of Fluids*, 34(3), 034117. Available from: <https://doi.org/10.1063/5.0085574>
- Neal, C.W.M. & Anders, A.M. (2015) Suspended sediment supply dominated by bank erosion in a low-gradient agricultural watershed, Wildcat Slough, Fisher, Illinois, United States. *Journal of Soil and Water Conservation*, 70(3), 145–155. Available from: <https://doi.org/10.2489/jswc.70.3.145>
- Nones, M. (2019) Dealing with sediment transport in flood risk management. *Acta Geophysica*, 67(2), 677–685. Available from: <https://doi.org/10.1007/s11600-019-00273-7>
- Osman, A.M. & Thorne, C.R. (1988) Riverbank stability analysis. I: Theory. *Journal of Hydraulic Engineering*, 114(2), 134–150. Available from: [https://doi.org/10.1061/\(ASCE\)0733-9429\(1988\)114:2\(134\)](https://doi.org/10.1061/(ASCE)0733-9429(1988)114:2(134))
- Over, J.S.R., Ritchie, A.C., Kranenburg, C.J., Brown, J.A., Buscombe, D.D., Noble, T., Sherwood, C.R., Warrick, J.A. & Wernette, P.A. (2021) Processing coastal imagery with Agisoft Metashape Professional Edition, version 1.6—Structure from motion workflow documentation (No. 2021–1039). US Geological Survey. <https://doi.org/10.3133/ofr20211039>
- Pedersen, A.N., Borup, M., Brink-Kjær, A., Christiansen, L.E. & Mikkelsen, P.S. (2021) Living and prototyping digital twins for urban water systems: towards multi-purpose value creation using models and sensors. *Water*, 13(5), 592. Available from: <https://doi.org/10.3390/w13050592>
- Prosser, I.P., Hughes, A.O. & Rutherford, I.D. (2000) Bank erosion of an incised upland channel by subaerial processes: Tasmania, Australia. *Earth Surface Processes and Landforms: the Journal of the British Geomorphological Research Group*, 25(10), 1085–1101. Available from: [https://doi.org/10.1002/1096-9837\(200009\)25:10<1085::AID-ESP118>3.0.CO;2-K](https://doi.org/10.1002/1096-9837(200009)25:10<1085::AID-ESP118>3.0.CO;2-K)
- Rachelly, C., Mathers, K.L., Weber, C., Weitbrecht, V., Boes, R.M. & Vetsch, D.F. (2021) How does sediment supply influence refugia availability in river widenings? *Journal of Ecohydraulics*, 6(2), 121–138. Available from: <https://doi.org/10.1080/24705357.2020.1831415>
- Rinaldi, M., Casaghi, N., Dapporto, S. & Gargini, A. (2004) Monitoring and modelling of pore water pressure changes and riverbank stability during flow events. *Earth Surface Processes and Landforms*, 29(2), 237–254. Available from: <https://doi.org/10.1002/esp.1042>
- Rinaldi, M., Mengoni, B., Luppi, L., Darby, S.E. & Mosselman, E. (2008) Numerical simulation of hydrodynamics and bank erosion in a river bend. *Water Resources Research*, 44(9), W09428. Available from: <https://doi.org/10.1029/2008WR007008>
- Sekely, A.C., Mulla, D.J. & Bauer, D.W. (2002) Streambank slumping and its contribution to the phosphorus and suspended sediment loads of the Blue Earth River, Minnesota. *Journal of Soil and Water Conservation*, 57(5), 243–250.
- Simon, A., Curini, A., Darby, S.E. & Langendoen, E.J. (2000) Bank and near-bank processes in an incised channel. *Geomorphology*, 35(3–4), 193–217. Available from: [https://doi.org/10.1016/S0169-555X\(00\)00036-2](https://doi.org/10.1016/S0169-555X(00)00036-2)
- Sjödahl, P., Dahlin, T., Johansson, S. & Loke, M.H. (2008) Resistivity monitoring for leakage and internal erosion detection at Hällby embankment dam. *Journal of Applied Geophysics*, 65(3–4), 155–164. Available from: <https://doi.org/10.1016/j.jappgeo.2008.07.003>
- Soil Scout. (2022) Soil Scout Hydra User Manual, accessed 29.8.2022, available online: [https://drive.google.com/file/d/0B4\\_CUFDRpZgXQnRPUGxTMGVbems/view?resourcekey=0-Lho5Og10zjSvXvPPFeHg](https://drive.google.com/file/d/0B4_CUFDRpZgXQnRPUGxTMGVbems/view?resourcekey=0-Lho5Og10zjSvXvPPFeHg)
- Spreitzer, G., Schalko, I., Boes, R.M. & Weitbrecht, V. (2022) Towards a non-intrusive method employing digital twin models for the assessment of complex large wood accumulations in fluvial environments. *Journal of Hydrology*, 614, 128505. Available from: <https://doi.org/10.1016/j.jhydrol.2022.128505>
- Stantzel, C., Kondolf, G.M., Schmitt, L., Combroux, I., Barillier, A. & Beisel, J.N. (2020) Restoring fluvial forms and processes by gravel augmentation or bank erosion below dams: a systematic review of ecological responses. *Science of the Total Environment*, 706, 135743. Available from: <https://doi.org/10.1016/j.scitotenv.2019.135743>
- Stroosnijder, L. (2005) Measurement of erosion: is it possible? *Catena*, 64(2–3), 162–173. Available from: <https://doi.org/10.1016/j.catena.2005.08.004>
- Tao, F., Xiao, B., Qi, Q., Cheng, J. & Ji, P. (2022) Digital twin modeling. *Journal of Manufacturing Systems*, 64, 372–389. Available from: <https://doi.org/10.1016/j.jmsy.2022.06.015>
- Thoma, D.P., Gupta, S.C., Bauer, M.E. & Kirchoff, C.E. (2005) Airborne laser scanning for riverbank erosion assessment. *Remote Sensing of Environment*, 95(4), 493–501. Available from: <https://doi.org/10.1016/j.rse.2005.01.012>
- Thorne, C.R. (1978) Processes of bank erosion in river channels. *PhD dissertation*.
- Thorne, C.R. (1981) Field measurements of rates of bank erosion and bank material strength. *Erosion and Sediment Transport Measurement (Proceedings of the Florence Symposium, June 1981)*, 133, 503–512. URL: [https://iahs.info/uploads/dms/iahs\\_133\\_0503.pdf](https://iahs.info/uploads/dms/iahs_133_0503.pdf)
- Tiusanen, J. (2005) Attenuation of a soil scout radio signal. *Biosystems Engineering*, 90(2), 127–133. Available from: <https://doi.org/10.1016/j.biosystemseng.2004.10.013>
- Tiusanen, M.J. (2013) Soil scouts: description and performance of single hop wireless underground sensor nodes. *Ad Hoc Networks*, 11(5), 1610–1618. Available from: <https://doi.org/10.1016/j.adhoc.2013.02.002>
- van Rooijen, E., Siviglia, A., Vetsch, D.F., Boes, R.M. & Vanzo, D. (2022) Quantifying fluvial habitat changes due to multiple subsequent

- floods in a braided alpine reach. *Journal of Ecohydraulics*, 1–21. Available from: <https://doi.org/10.1080/24705357.2022.2105755>
- Vandermause, R., Harvey, M., Zevenbergen, L. & Ettema, R. (2021) River-ice effects on bank erosion along the middle segment of the Susitna river, Alaska. *Cold Regions Science and Technology*, 185, 103239. Available from: <https://doi.org/10.1016/j.coldregions.2021.103239>
- Veihe, A., Jensen, N.H., Schiøtz, I.G. & Nielsen, S.L. (2011) Magnitude and processes of bank erosion at a small stream in Denmark. *Hydrological Processes*, 25(10), 1597–1613. Available from: <https://doi.org/10.1002/hyp.7921>
- Verdonen, M., Störmer, A., Lotsari, E., Korpelainen, P., Burkhard, B., Colpaert, A. et al. (2023) Permafrost degradation at two monitored palsas in north-west Finland. *The Cryosphere*, 17(5), 1803–1819. <https://doi.org/10.5194/tc-17-1803-2023>
- Weller, A., Lewis, R., Canh, T., Möller, M. & Scholz, B. (2014) Geotechnical and geophysical long-term monitoring at a levee of Red River in Vietnam. *Journal of Environmental and Engineering Geophysics*, 19(3), 183–192. Available from: <https://doi.org/10.2113/JEEG19.3.183>
- Wilson, G.V., Periketi, R.K., Fox, G.A., Dabney, S.M., Shields, F.D. & Cullum, R.F. (2007) Soil properties controlling seepage erosion contributions to streambank failure. *Earth Surface Processes and Landforms: the Journal of the British Geomorphological Research Group*, 32(3), 447–459. Available from: <https://doi.org/10.1002/esp.1405>
- Wynn, T.M., Henderson, M.B. & Vaughan, D.H. (2008) Changes in streambank erodibility and critical shear stress due to subaerial processes along a headwater stream, southwestern Virginia, USA. *Geomorphology*, 97(3–4), 260–273. Available from: <https://doi.org/10.1016/j.geomorph.2007.08.010>
- Yumoto, M., Ogata, T., Matsuoka, N. & Matsumoto, E. (2006) Riverbank freeze-thaw erosion along a small mountain stream, Nikko volcanic area, central Japan. *Permafrost and Periglacial Processes*, 17(4), 325–339. Available from: <https://doi.org/10.1002/ppp.569>
- Zhang, Q., Gu, X., Singh, V.P., Shi, P. & Luo, M. (2017) Timing of floods in southeastern China: seasonal properties and potential causes. *Journal of Hydrology*, 552, 732–744. Available from: <https://doi.org/10.1016/j.jhydrol.2017.07.039>

## SUPPORTING INFORMATION

Additional supporting information can be found online in the Supporting Information section at the end of this article.

**How to cite this article:** van Rooijen, E., Dietze, M. & Lotsari, E. (2023) Employing novel wireless agricultural sensors for real-time monitoring of fluvial bank erosion. *Earth Surface Processes and Landforms*, 48(13), 2480–2499. Available from: <https://doi.org/10.1002/esp.5640>